Environmental Science & Technology
Critical Review
Cite This: *Environ. Sci. Technol.* 2018, 52, 381−396
pubs.acs.org/est

Review of the Scientific Understanding of Radioactive Waste at the U.S. DOE Hanford Site

Reid A. Peterson,*,† Edgar C. Buck,† Jaehun Chun,‡ Richard C. Daniel,† Daniel L. Herting,§ Eugene S. Ilton,‡ Gregg J. Lumetta,† and Sue B. Clark†,⊥

†Energy and Environment Directorate and ‡Physical and Computational Science Directorate, Pacific Northwest National Laboratory, Richland, Washington 99352, United States

§Washington River Protection Solutions, Richland, Washington 99354, United States

⊥Chemistry Department, Washington State University, Pullman, Washington 99164, United States

ABSTRACT: This Critical Review reviews the origin and chemical and rheological complexity of radioactive waste at the U.S. Department of Energy Hanford Site. The waste, stored in underground tanks, was generated via three distinct processes over decades of plutonium extraction operations. Although close records were kept of original waste disposition, tank-to-tank transfers and conditions that impede equilibrium complicate our understanding of the chemistry, phase composition, and rheology of the waste. Tank waste slurries comprise particles and aggregates from nano to micro scales, with varying densities, morphologies, heterogeneous compositions, and complicated responses to flow regimes and process conditions. Further, remnant or changing radiation fields may affect the stability and rheology of the waste. These conditions pose challenges for transport through conduits or pipes to treatment plants for vitrification. Additionally, recalcitrant boehmite degrades glass quality and the high aluminum content must be reduced prior to vitrification for the manufacture of waste glass of acceptable durability. However, caustic leaching indicates that boehmite dissolves much more slowly than predicted given surface normalized rates. Existing empirical models based on ex situ experiments and observations generally only describe material balances and have not effectively predicted process performance. Recent advances in the areas of in situ microscopy, aberration-corrected transmission electron microscopy, theoretical modeling across scales, and experimental methods for probing the physics and chemistry at mineral−fluid and mineral−mineral interfaces are being implemented to build robustly predictive physics-based models.

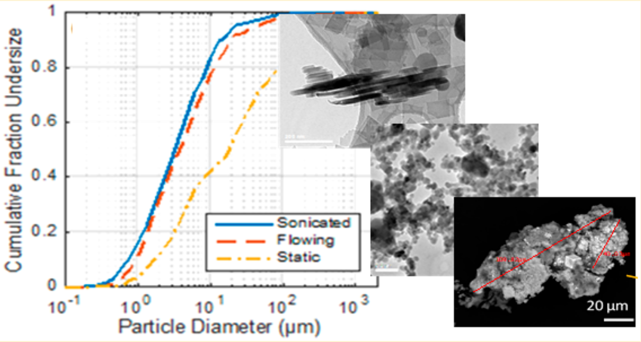

■ INTRODUCTION

The U.S. Department of Energy (DOE) Hanford Site in Washington State is home to 177 underground storage tanks containing 56 million gallons of mixed radioactive and chemical waste from the processing of irradiated fuel for the recovery of plutonium for nuclear weapons. This site has been referred to as "the most toxic place in America."[1] The Hanford tank wastes are chemically complex, having been largely generated during three major plutonium separation operations over a period of 40 years. The current projected cost for the DOE facility to remediate the Hanford tank waste exceeds \$16B, just a portion of the \$110B projected cost to remediate the Hanford Site. The deployment of these processes has been delayed several times, resulting in increasing budgets and delayed completion. The total environmental management cost represents the third largest federal liability behind Social Security and Medicare.

The tank waste will be partitioned into high-level waste (HLW) and low-activity waste (LAW). The LAW will be pretreated to remove ^{137}Cs, and then immobilized in borosilicate glass for on-site storage. The HLW will be pretreated to lower the concentrations of Al, Cr, Na, P, and S, which negatively affect vitrification,[2] and then immobilized in a borosilicate glass matrix, cast into stainless steel canisters, and placed in a geological repository.

Hanford tank waste is categorized according to three general types: (1) supernatant liquid, (2) saltcake solids, and (3) sludge. The primary distinction between saltcake and sludge is the proportion of sparingly soluble material (sludge) versus soluble salt phases. The saltcake phase is expected to dissolve quickly during the initial sluicing of the wastes with water during retrieval. The supernatant liquid, combined with the dissolved salt solution, constitutes the LAW fraction (after removal of the ^{137}Cs). The water-insoluble sludge constitutes the HLW fraction. There is particular interest in the nanosize particulates that are difficult to characterize or define, but owing to their small size and propensity to aggregate, have a large influence on sludge rheology.

Received: August 8, 2017
Revised: November 20, 2017
Accepted: December 7, 2017
Published: December 7, 2017

DOI: 10.1021/acs.est.7b04077

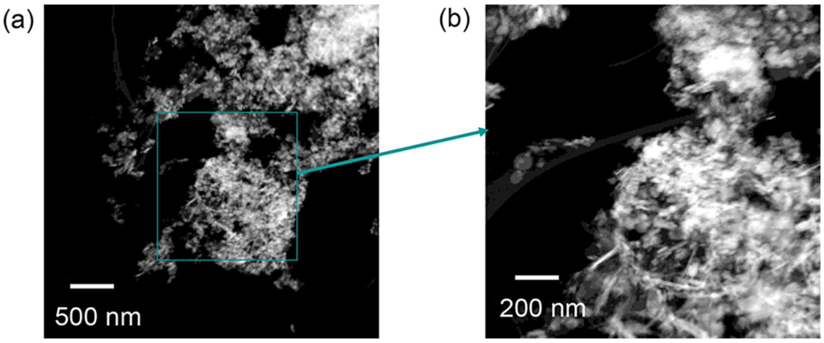

Figure 1. STEM images of REDOX sludge (see text).[3]

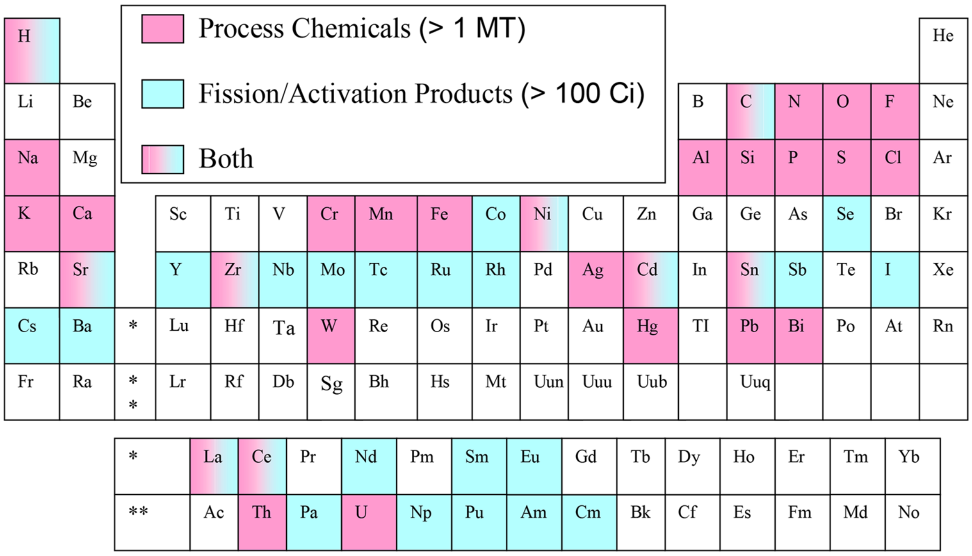

Figure 2. Elements and radionuclides present in significant quantities in tank waste.

In an effort to develop effective methods for treating tank waste, its physical and chemical characteristics have been investigated. This Critical Review reviews the most relevant macroscopic and microstructural information available to date, with an emphasis on the sludge fraction that contains the highest concentrations of the sparingly soluble phases that drive waste processing operations. Indeed, nearly all of the issues delaying treatment of these wastes are associated with the sparingly soluble fraction, either in the development of mixing and transfer systems or in the potential for these materials to accumulate at different stages of the proposed processes. In the first and second sections of this paper, we review the history and general character of tank waste, then summarize the processes that created the waste. The third section outlines emergent physical and chemical behaviors of tank waste with an emphasis on issues related to waste processing for ultimate disposal. In the fourth and fifth sections, we highlight the complexity of tank waste at the micro- to nanoscale and aggregate scale that underlies much of its often baffling macroscopic behavior with select examples. In the final section, in contrast to the usual reliance on phenomenological models, we make the case that predicting and controlling tank waste behavior requires quantitative information on the physics and chemistry of particle-fluid interfaces as well as higher spatial and chemical resolution of the solid phase. A few examples are provided that highlight recent progress toward this goal. In this regard, there is a renewed energy and incentive for building physics/chemistry-based predictive models of tank waste behavior enabled by recent developments in electron and atomic force microscopy.

■ OVERVIEW OF THE HISTORY AND CHARACTERIZATION OF TANK WASTE

The Hanford tanks possess extremely complex and diverse waste compositions, because of (1) the number of different separation techniques used at Hanford for plutonium recovery, (2) waste transfers made to optimize tank utilization, (3) addition of other materials from auxiliary processes, (4) radionuclide-induced self-heating that caused boiling of the waste in some instances, and (5) in situ coprecipitation of medium-lived radioisotopes (e.g., ^{90}Sr). The resulting tank sludge solids are highly heterogeneous in composition, structure and phase, morphology, and particle size. Scanning transmission electron microscopy (STEM) images[3] of finely intermixed uranium and transition metal (oxyhydr)oxides illustrate this complexity (Figure 1). The particles are agglomerated and irregularly shaped. Much of the material is extremely small but there are also large particles. This type of material presents an enormous challenge for modelers trying to predict the rheological behavior of the wastes, which in turn affects the rate at which the wastes can be treated for disposal.

The complexity of waste composition is partly responsible for the common misperception that the composition of the waste in the Hanford Site underground storage tanks is a mystery. Terms like "witch's brew" are often used to describe the tank contents. Another common misperception is that Hanford tank waste contains every element in the periodic table. Figure 2 shows a color-coded periodic table that includes all of elements in tank waste that derive from the process chemicals (in amounts greater than 1 t) and all of the radionuclides (in amounts greater than 3.7 TBq) derived from fission and activation products.

The Best Basis Inventory[4] is an active public-access database that tracks the total Hanford tank inventory of 25 chemical constituents and 46 radionuclides and their distribution among the 177 individual tanks. These chemical constituents and radionuclides represent over 99% of the total inventory. Data come from four sources: sample analysis (preferred); direct calculations (i.e., correlation of one analyte with another, e.g., ^{90}Y derived from ^{90}Sr); engineering estimates (pre-1989 analyses and process knowledge); and waste type templates, either model-based[5] or sample-based.

Although the composition of the waste streams transferred from the processing plants to the storage tanks was well documented (e.g., Klem[6]), matters became complicated due to subsequent waste management activities (crib disposal, trench disposal, evaporation, salt well pumping, and others) that were implemented to recover tank storage space. Because these procedures required tank-to-tank transfers of waste, and tank waste is not homogeneous, the composition of the waste in the source and destination tanks became more uncertain with each transfer.

Sampling of the underground storage tanks was not a routine activity until the early 1970s, at which time methods were developed for taking "dip" samples from tanks. Core sampling of single-shell tanks began in 1985. Some of the analytical methods were not reliable, and routine methods for chemical analysis of tank waste sampling required a period of development, whereas analytical protocols for radionuclides were established. However, most of the current analytical methods were developed and in place before 1989, the year in which the Hanford Federal Facility Agreement and Consent Order[7] was signed. (We note that if you do not have a PNNL or HLAN account, ref 7 is available by request.) In fact, the Tank Waste Information System (TWINS) database has separate tables for pre- and post-1989 sample analyses, but the Best Basis Inventory[4] calculation uses only the post-1989 sample results.

Supernate (or supernatant liquor) is the aqueous liquid phase that typically resides atop the sludge or saltcake and is usually retrieved from the tank via "grab samples", that is, lowering a glass bottle into the supernate layer, remotely removing the stopper from the bottle, and then retrieving the full bottle. Typical supernate is a concentrated aqueous solution of (primarily) sodium salts, including sodium nitrate, nitrite, hydroxide, aluminate, carbonate, phosphate, sulfate, fluoride, oxalate, and others. An average total sodium concentration is about 11 mol/L with an average density around 1.4 g/mL and pH > 12.

Saltcake is a mixture of water-soluble solids and "interstitial liquid" occupying the pores in between the particles. The interstitial liquid usually has the same composition as the supernate. Sodium nitrate is the most common solid phase, though the mineralogy varies significantly among tanks. Other common solids include sodium carbonate (trona), sodium phosphate, sodium fluoride phosphate (natrophosphate), sodium oxalate, and other sodium salts. Potassium salts can be present, but at much lower concentrations. Saltcake samples are obtained by core sampling.

Sludge is a mixture of water-insoluble solids and interstitial liquid. The insoluble solids were formed initially in the processing plants by neutralization of the acidic processing solutions containing mixed metal nitrates. The solids are largely amorphous agglomerates containing oxides/hydroxides of aluminum, iron, silicon, bismuth, chromium, and other metals. Crystalline phases have been identified including gibbsite [$Al(OH)_3$], boehmite [γ-AlOOH], dawsonite [$NaAlCO_3(OH)_2$], cancrinite [$Na_3CaAl_3Si_3O_{12}CO_3$], thermonatrite [$Na_2CO_3 \cdot H_2O$], natrophosphate [$Na_7F(PO_4)_2 \cdot 19H_2O$], hematite [$Fe_2O_3$], and clarkeite [$Na((UO_2)O(OH))(H_2O)_{0-1}$].[8,9] Sludge samples are obtained by core sampling, though other methods (e.g., "clam shell" and "finger trap") have been utilized, especially for tank heels.

A full analytical suite for the three waste types is listed below. Quantitative wet chemistry determination of sludge solid phase compositions involves a dissolution step using acid or molten KOH, whereas salt-cake solids are dissolved in water.

- Inductively coupled plasma analysis for metals (Na, Al, Fe, Si, and approximately 30 other metals).
- Ion chromatography analysis for anions (hydroxide, nitrate, nitrite, phosphate, sulfate, oxalate, chloride, acetate, glycolate, formate).
- Total inorganic carbon/total organic carbon; inorganic carbon is assumed to derive exclusively from carbonate ion; organic carbon derives from a variety of sources, but is often dominated by oxalate.
- Thermogravimetric analysis (TGA) for determination of weight percent water; sometimes measured by oven-drying rather than by TGA.
- Free hydroxide (hydroxide ion not bound to metal ions).
- Density.
- Rheology (typically measured using a concentric cylinder or falling ball rheometer).
- Particle size distribution (PSD; typically measured by laser diffraction).
- Solid-phase characterization (polarized light microscopy/scanning electron microscopy (SEM)/transmission electron microscopy (TEM)/X-ray diffraction (XRD)).
- Radiochemistry (total alpha, total beta, alpha energy analysis, gamma energy analysis).

■ ORIGINS OF THE TANK WASTE

To better understand the nature of the alkaline radioactive tank waste, it is helpful to have a basic understanding of the Pu separation processes that generated the waste. Three major Pu separation processes were implemented at the Hanford Site: (1) the bismuth phosphate process (BiPP), (2) the reduction−oxidation (REDOX) process, and (3) the plutonium uranium reduction extraction (PUREX) processes. The Savannah River Site (SRS) used PUREX almost exclusively. Variants of PUREX were implemented for ^{239}Pu (primarily separated from U-based fuel) versus ^{238}Pu (primarily separated from the ^{237}Np target) production. A number of auxiliary processes were implemented at Hanford that either produced additional waste or significantly altered the original waste streams. Most of these processes began by separating the irradiated metallic U fuel from the Al cladding by dissolving the Al cladding in an aqueous mixture of NaOH and $NaNO_3$. Following removal of the decladding solution, the exposed metallic fuel was dissolved in hot HNO_3.

The Bismuth Phosphate Process. The BiPP exploits the fact that actinides in the +4 oxidation state preferentially partition from solution into a $BiPO_4$ precipitate, whereas actinides in the +5 and +6 oxidation states remain in solution. This method was used to separate Pu from U, other transuranium elements (i.e., Np and Am), and fission product elements by shuttling the Pu between the +4 and +6 oxidation states. Although conceptually simple, the BiPP required substantial process chemicals, leading to a large mass of waste. The major metallic elements entering the waste were Al, Bi, Fe, Ce, Cr, K, La, Mn, Na, Si, and Zr. Anionic species included nitrate, nitrite, fluoride, phosphate, sulfate, and hydroxide. The bulk U from the fuel itself also was included in the waste stream from the BiPP, but the wastes that were rich in U were retrieved later and processed to recover U as described later.

The REDOX Process. The REDOX process was the first liquid−liquid extraction method for recovery of Pu from irradiated U fuel. Further, in contrast to the BiPP, U was captured for reuse. The REDOX process utilized the fact that tetravalent and hexavalent actinides partition into methyl isobutyl ketone (hexone in Hanford historical documents) in the presence of a salting-out reagent, whereas trivalent Pu has little affinity for the organic phase.

The REDOX process, unlike other aqueous-based fuel reprocessing schemes, was operated at a very low HNO_3 concentration because of the acid-instability of the methyl isobutyl ketone solvent. There were two major consequences of this low-acid flowsheet. First, it was necessary to maintain an excess of $Na_2Cr_2O_7$ through most of the process to keep the Pu in the +6 oxidation state. Reduction of Pu to +4 under low acid conditions would have led to the formation of an unextractable Pu(IV) polymeric species.[10] Second, large amounts of $Al(NO_3)_3$ were required as source of nitrate to promote extraction of U and Pu into the organic phase. Consequently, REDOX process wastes are high in Cr and Al. The basic REDOX process steps were (1) oxidation of Pu to +6 with $Na_2Cr_2O_7$, (2) addition of $Al(NO_3)_3$, (3) coextraction of Pu(VI) and U(VI) into methyl isobutyl ketone, (4) scrubbing of the loaded organic phase with an $Al(NO_3)_3$ solution containing $Na_2Cr_2O_7$ to remove most coextracted fission products, (5) stripping of Pu from the organic phase by contact with and aqueous phase containing iron(II) sulfamate (to reduce the Pu to the unextractable +3 state) and $Al(NO_3)_3$ (to maintain a high U distribution ratio), and (6) stripping of the U into water or dilute HNO_3. Repeated extraction cycles were performed on the Pu and U streams to increase purity. Major metallic elements entering the waste tanks included Al, Cr, K, Mn, and Na. Anionic species introduced included nitrate, nitrite, sulfate, and hydroxide.

The PUREX Process. The PUREX process is the worldwide standard in recovering Pu and U from irradiated nuclear fuel.[11] PUREX became the main Pu production process used at Hanford after its introduction in 1956. The method, described in detail by Clark et al.,[12] extracts Pu(IV) and U(VI) from a nitric acid solution into a hydrocarbon phase containing tributyl phosphate (TBP):

$$\begin{aligned} &Pu^{4+}(aq) + 4NO_3^-(aq) + 2TBP(org) \\ &\quad \rightleftharpoons Pu(NO_3)_4(TBP)_2(org) \end{aligned} \tag{1}$$

$$\begin{aligned} &UO_2^{2+}(aq) + 2NO_3^-(aq) + 2TBP(org) \\ &\quad \rightleftharpoons UO_2(NO_3)_2(TBP)_2(org) \end{aligned} \tag{2}$$

Pu is then separated from U by reducing the Pu to the +3 oxidation state which is not soluble in TBP. The primary Pu reductant used at both Hanford and SRS was iron(II) sulfamate. This reductant indirectly stabilized Pu in the +3 oxidation state by scavenging nitrous acid in order to slow the reoxidation of Pu to +4 by nitrate ion.[10,13]

$$HNO_2 + NH_2SO_3^- \rightarrow N_2 + H_2O + H^+ + SO_4^{2-} \tag{3}$$

Consequently, the PUREX process introduced Fe and sulfate into the tank waste. Hydroxylamine nitrate was also used as a Pu reductant and nitrous acid scavenger both at Hanford and SRS.[14]

The PUREX process was also applied to fuel from the Hanford Site N-Reactor, which was clad in Zircaloy. The Zircaloy cladding was dissolved in a boiling solution of ammonium fluoride and ammonium nitrate (the Zirflex process; see Swanson[15]). This resulted in the so-called neutralized cladding removal waste, which contains large amounts of Zr and F.

The PUREX process substantially reduced the HLW volume compared to the earlier BiPP and REDOX Pu extraction processes. The use of HNO_3 as the salting-out agent instead of $Al(NO_3)_3$ reduced both nitrate and Al waste streams; HNO_3 was easily and economically recovered and recycled. Further, the use of oxidants such as $Na_2Cr_2O_7$ was greatly reduced. The primary sources of chemical wastes generated during PUREX operations were cladding waste, Fe, sulfate, $NaNO_2$, and $NaNO_3$ from neutralization of the acidic wastes with NaOH prior to transfer to the underground storage tanks.

Uranium Recovery Process. The uranium recovery process implemented in the 1950s had three primary functions: (1) recovery of the U-bearing waste from the storage tanks, (2) separation of U from the waste, and (3) conversion of the separated U to UO_3. The U that was recovered from the waste tanks as well the U produced in the REDOX process were used as feed for the UO_3 Plant.[16]

In brief, the U-bearing waste in the underground storage tanks was mixed with the alkaline supernatant liquid to form a slurry. The slurry was pumped into an underground vault and then fed into a tank containing HNO_3. The acidified waste and solubilized U was then pumped to the Hanford TBP Plant (221-U Building) for processing. After adjustment of the feed to ~3 mol/L HNO_3 and clarification by centrifugation, U was extracted into TBP dissolved in a hydrocarbon diluent (process developed at Oak Ridge National Laboratory[17]). The primary difference between PUREX and the U recovery operation was the inclusion of iron(II) sulfamate in the scrub stream so that the uneconomical amount of Pu still present was reduced to the poorly extractable +3 state in the extraction column and exited the column in the aqueous high activity waste stream. The resulting high-activity waste stream was neutralized, concentrated by evaporation, and returned to the underground waste storage tanks.

The U recovery process contributed the following process chemicals to Hanford tank waste: (1) $NaNO_3$ resulting from reneutralization of the high-activity waste stream, (2) iron from the iron(II) sulfamate used as Pu reductant, and (3) sulfate from iron(II) sulfamate and Na_2SO_4 used during cleanup of the TBP solvent.

Strontium and Cesium Separations. Strontium-90 ($t_{1/2}$ = 28.6 y) and ^{137}Cs ($t_{1/2}$ = 30.2 y) are major contributors to the heat generated from nuclear fission wastes. These isotopes also have potential commercial value—^{90}Sr as a source of ^{90}Y used in medical applications,[18−20] and ^{137}Cs as a source of γ rays (through decay of its daughter $^{137\text{m}}$Ba, which emits a 662 keV γ ray) for sterilization applications.[21] Megacuries of these two isotopes have been separated from acidic process solutions and from tank waste at Hanford.[22]

During the 1950s, ^{137}Cs (as well as ^{90}Sr to some extent) was removed from the alkaline tank waste supernatant liquids by precipitation with nickel ferrocyanide.[23] Sodium ferrocyanide and strontium nitrate were added to the acidic process solutions. Sodium hydroxide and nickel sulfate were then added to adjust the solution pH to a target of 9.5; nickel ferrocyanide and $Sr(OH)_2$ precipitated carrying down ^{137}Cs and ^{90}Sr, respectively. The resulting slurry was transferred to the underground storage tank and the solids given time to settle. The clarified liquid was then discharged to ground in so-called “cribs” in order to expand available tank space. The possible presence of ferrocyanide in the tank waste has raised safety concerns regarding potential energetic reactions that might occur if the tank wastes were to dry out. This issue was eventually resolved by Cash et al.[24]

From 1967 to 1969, ^{137}Cs was removed from Hanford tank waste liquids at B Plant using cation exchange technology,[25] including the zeolite ion exchangers and a phenolic-based organic resin. Approximately 4×10^8 Bq of ^{137}Cs was recovered from 2×10^8 L of Hanford Site wastes during these campaigns.

Strontium-90 was recovered at the Hanford Hot Semi-works[26] and at B Plant.[27] Sr^{2+} was extracted from acetate-buffered solutions at pH 4.7 into an organic phase containing di-2-ethylhexylphosphoric acid (HDEHP) dissolved in a hydrocarbon diluent. TBP was added as a phase modifier to prevent formation of a third liquid phase in the system. Complexants, such as ethylenediaminetetraacetic acid (EDTA) and diethylenetriaminepentaacetic acid (DTPA), were added to complex higher valent ions, such as Fe^{3+} and various transuranics, to (1) prevent their hydrolysis and precipitation and (2) suppress their extraction by HDEHP. These species were eventually routed to waste tanks and are important components of the complexant concentrate (CC) waste. The CC waste now provides unique challenges due to hydrogen production from radiolytic degradation of the organics, and high concentrations of transuranic elements that would normally reside in the solid sludge phase.

EMERGENT PHYSICAL AND CHEMICAL PROPERTIES OF HANFORD TANK WASTE

Thermodynamics and Chemical Processing. Thermodynamic modeling, or empirically derived solubilities, has long been used to determine saturation states of tank liquids and chemically processed waste at Hanford. Early work that applied empirically derived solubilities or the so-called “Barney diagram” to tank waste showed that Al phase solubilities for a given pH could not be extrapolated to different ionic strengths and were not accurately predicted by the available thermodynamic models based primarily on dilute solution theory (Reynolds and Reynolds[28] and references therein).

As more advanced thermodynamic approaches applicable over a broader range of ionic strength became available, they were used to model solid−fluid equilibria in conjunction with tank fluid and solid phase information. The first advanced thermodynamic modeling efforts used the ESP simulation package from OLI Systems Inc.[29] In 2005, solubility data for double salts were included in the database.[30,31] Over the same period, Felmy and co-workers used the more comprehensive Pitzer thermodynamic modeling approach to predict saturation states in tank wastes and stimulants.[32−37] This approach was adopted by Jacob Reynolds and co-workers,[38−40] who also expanded the database. Input data that have not been adequately addressed, however, include the effect of size, degree of crystallinity, and possible solid solution on particle stability. As shown in the section on microanalysis, all these complications are present in tank wastes.

An important goal is to predict how tank waste chemistry will respond to waste processing conditions that include increasing temperature and base concentrations, and addition of other additives. Whereas empirically derived solubilities are still used, they are expensive, and the hope is that they will be replaced by modeling. However, all of the models in use to describe proposed operations are equilibrium based, whereas chemical processing is a nonequilibrium process by definition. Including kinetic models of phase dissolution or precipitation within the current equilibrium models would be a major step forward.

Allowing that tank conditions are changing, including decreasing radiation fields, such that equilibrium is a moving target, it is a truism that equilibrium will eventually prevail. In contrast, kinetics are highly sensitive to extrinsic factors such as the flow regime and extent of mixing (i.e., hydrodynamics) and solid phase characteristics such as morphology, the expression of reactive surfaces, surface coatings and complexes, and aggregation. Outstanding issues, given that the tank wastes have been around for more than half a century, include the oversaturation of gibbsite and the persistence of nanoparticles and amorphous/low crystalline materials. With respect to chemical processing, a critical step is caustic dissolution of gibbsite and boehmite, yet tank waste boehmite dissolves 40 times more slowly than predicted for surface normalized rates.[41] Experiments that simulate tank waste or use actual tank waste, coupled to in situ and ex situ microscopy and spectroscopy, would help tease apart thermodynamic and kinetic factors. Given the complexity and expense, a rational path forward is to use simplified systems informed by microanalysis of tank waste. An example of this approach is given in a later section.

Rheology. The rheology of Hanford wastes has been measured to support the design of waste slurry handling systems (e.g., pumps and mixers).[8,42−66] Results have been summarized by Wells et al.[8,53] and Meacham et al.[67] The rheology of the liquid and supernate fractions is Newtonian, as the soluble species are typically limited to simple sodium salts (such as sodium hydroxide, phosphate, nitrate, nitrite, carbonate, and sulfate). However, given the high degree of saturation, small perturbations could promote precipitation and a more complex rheology. Given the simpler case, that is, no precipitation, empirical correlations between the liquid viscosity and density have found some success.[8,53,67] The most recent correlation[67] is

$$\mu_L = \exp\left[aq + b(\rho_L - 1) + \frac{c(\rho_L - 1) + d}{T}\right] \tag{4}$$

where μ_L is the liquid viscosity in mPa s, ρ_L is the liquid density in g mL^{-1}, and T is the liquid temperature in K. The term q depends on liquid density and is given by

$$q = \begin{cases} (\rho_L - 1) & \text{if } (\rho_L - 1) \geq 0 \\ 0 & \text{if } (\rho_L - 1) < 0 \end{cases} \qquad (5)$$

The constants a, b, c, d, and f were determined by linear-regression analysis, and are 5.29, −18.29, 7103.79, 54.36, and 1.42, respectively.[67] As illustrated in Figure 3, eq 4 works well at relatively low viscosities, but becomes unpredictive at higher viscosities (experimental data from Wells et al.[8]).

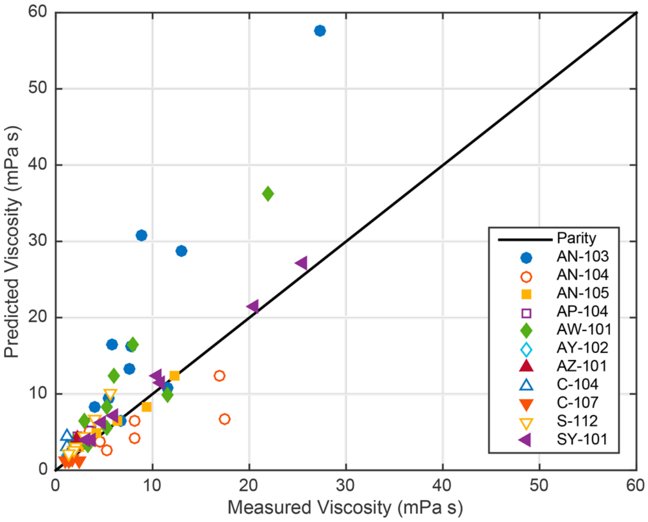

Figure 3. Parity plot showing the predictive performance of eq 1 against liquid rheology data reported in Wells et al.[8]

The Hanford waste slurries exhibit both Newtonian and non-Newtonian rheology, with the latter treated by several constitutive models including the Bingham-plastic, Casson, and Power-Law models. Measured Bingham-plastic yield stress and consistency as a function of undissolved solids content for Hanford sludge and saltcake wastes are shown in Figure 4; note the broad range of values and the lack of correlation between the mass fraction and both the yield stress and consistency. Currently, no general correlation predicts Hanford sludge and saltcake slurry rheology; very limited success has been restricted to measurements for a single tank and/or waste type using highly simplified correlations (e.g., see waste slurry fits in Wells et al.[53]).

The development of predictive models with robust and general correlations requires a fundamental understanding of the forces between and particle morphologies, compositions, and size. In this regard, the next two sections summarize our current knowledge of Hanford tank solids.

■ MICROANALYSIS OF HANFORD TANK SOLIDS

Compilations of phases identified in the Hanford tank waste are given in Herting and Cooke,[68] Lumetta et al.,[69] and Wells et al.[8,53] Here, we highlight the more abundant sparingly soluble phases that strongly influence the rheology and other aspects of waste processing operations. Attention is also paid to radioactive material that influences decisions concerning classification as HLW or LAW, and that poses potential threats to operational safety. The focus is on sludge particles that are sparingly soluble, whereas saltcake phases are not considered a problem as they dissolve upon sluicing operations. Obviously, a primary goal has been to simply identify solid phases. However, to evaluate the origin of emergent properties, it is also necessary to determine phase compositions, degrees of crystallinity, morphology, particle size, and aggregate characteristics. Table 1 displays triangular PSDs for phases observed in sludge based on the analysis performed by Wells et al.[39] Such information will allow better prediction of settling rates, dissolution rates and extent, rheology, and filtration rates that impact liquid−solid phase separation steps that follow dissolution. For example, how fast a phase settles can become a critical issue during transfer or pumping of tank waste, yet many so-called pure phases are embedded in low-crystalline/amorphous material. Further, nontrivial rheological behavior that cannot be estimated from a simple linear correlation[70] can result from the interaction of nanoscale and micron sized particles due to the unique nature of nanoparticle interactions.[71,72] Characterizing samples after caustic leaching and prior to pumping the waste to the vitrification plant is also necessary in order to determine potential altered properties due, in part, to incongruent dissolution.

In REDOX-derived wastes, the major less-soluble crystalline phases detected by XRD in the sludge include aluminum (oxy)hydroxides (gibbsite, boehmite, and dawsonite); Al-silicates (cancrinite); iron (hydr)oxides (hematite and ferrihydrite); uranium oxides (sodium uranate and uranyl phosphates); and chromium and zirconium oxides. Broad peaks and background features indicate nanosize particles and an appreciable proportion of amorphous or poorly crystalline

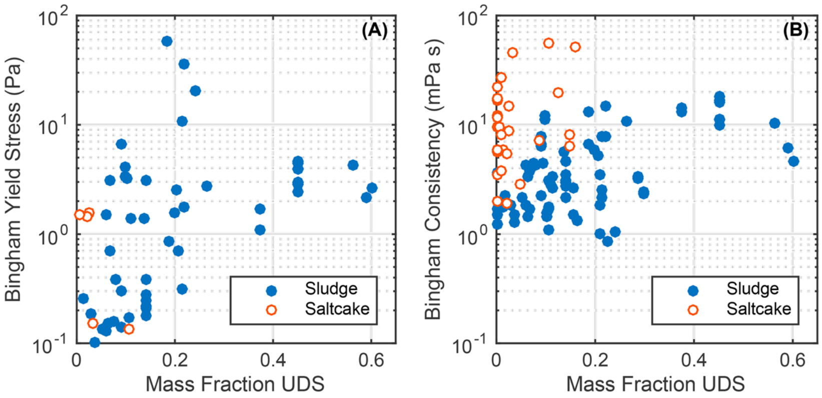

Figure 4. Summary of "best-fit" Bingham yield stress (A) and consistency (B) for Hanford wastes as a function of the mass fraction of undissolved solids (UDS) at 25 °C.

Table 1. Summary of Phases Observed in Sludge and Size Distributions (from Wells et al.[53])

Mol. Formula	Mineral Name/Description	Triangular Distribution of Primary Particles (μm)		
Ag	metallic silver (alloy with Hg)	2		
Ag_2O	silver oxide	2		
Bi_2O_3	Bismite	3	1	1
$BiFeO_3$	bismuth iron silicate-phosphate (bismutoferrite related)	0.1	0.06	0.035
$Ca_5OH(PO_4)_3$	apatite-related phase	9		0.05
$CaCO_3$	Calcite	55		
CaF_2		15		
CrOOH [**b**]	mixed Al-Cr oxide phase	0.4	0.1	0.02
FeOOH	Iron Oxide	0.015	0.01	0.005
$Al(OH)_3$	Gibbsite	200		0.8
Al(O)OH [**d**]	Boehmite	0.052	0.048	0.015
$LaPO_4•2H_2O$	lanthanum phosphate	3	0.2	0.1
$Mn_3(PO_4)_2$	Sidorenkite	8		8
MnO_2	Birnessite	10	1.3	0.3
$Na_2(UO_2)_2(PO_4)_2•2H_2O$	sodium uranyl phosphate (autunite related)	5		
$Na_2U_2O_7$ / U_3O_8	clarkeite, oxide	5	0.1	0.05
$NaAlCO_3(OH)_2$	Dawsonite	4.2	0.94	0.14
$Na_{7.6}[AlSiO_4]_6(NO_3)_{1.6}•(H_2O)_2$ $(NaAlSiO_4)$	NO_3-cancrinite	8	2.5	1
$Ni(OH)_2$	nickel hydroxide	0.5	0.2	0.005
$PbCO_3$	Cerussite	5		
PuO_2		20	4	0.5
SiO_2	quartz	100		
$Sr_3(PO_4)_2$	apatite' related phase	0.065	0.045	0.02
ZrO_2	Zirconia	50	0.2	0.05
Ag_2CO_3	silver carbonate	2		
Al-Silicates	“zeolites”	20	5	0.1
Al-Silicates	“clays”	0.6	0.3	0.1
$BiPO_4$	bismuth phosphate	10	2	1
Fe_2O_3	Hematite	1.6	0.88	0.037
$Na_4(UO_2)(CO_3)_3$	Cejkaite	50	7.5	2
$Pb_5(OH)(PO_4)_3$	Pyromorphite	0.4		0.05
ZrOOH	zirconium hydroxide	10		

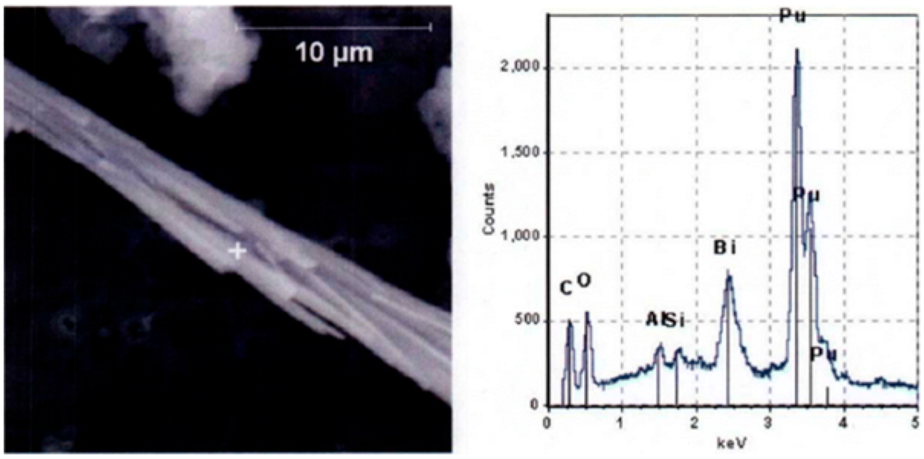

Figure 5. SEM image and energy dispersive X-ray spectroscopy (EDS) spectrum of a representative a Pu−Bi−O rich particulate. Such a phase could have a significant effect on waste processing safety (see text). Figure 5 is reprinted by permission from Springer Nature, *Journal of Radioanalytical and Nuclear Chemistry*, Discovery of plutonium−bismuth and plutonium−bismuth−phosphorus containing phases in a Hanford waste tank, J. G. Reynolds, G. A. Cooke, J. K. McCoskey et al., 2016.[74]

solids. In contrast, phase identification in the BiPP waste has been less definitive where unique compositions yielded unusual material not well described or documented in the literature.

In addition to XRD, discussed earlier, sludge has also been characterized by electron and X-ray microscopy and spectroscopy. An important example of the need for electron microscopy is the discovery by Reynolds and co-workers[73,74] of plutonium−bismuth and plutonium−bismuth−phosphate phases (Figure 5). Although relatively uncommon, these Pu containing particles are of great concern because they are large (tens of microns long) and likely dense, and could potentially gravity segregate during waste processing. Because the estimated inventory of Pu in the Hanford tank waste is on the order of 10^5 g,[75] there is a risk that enough Pu-containing

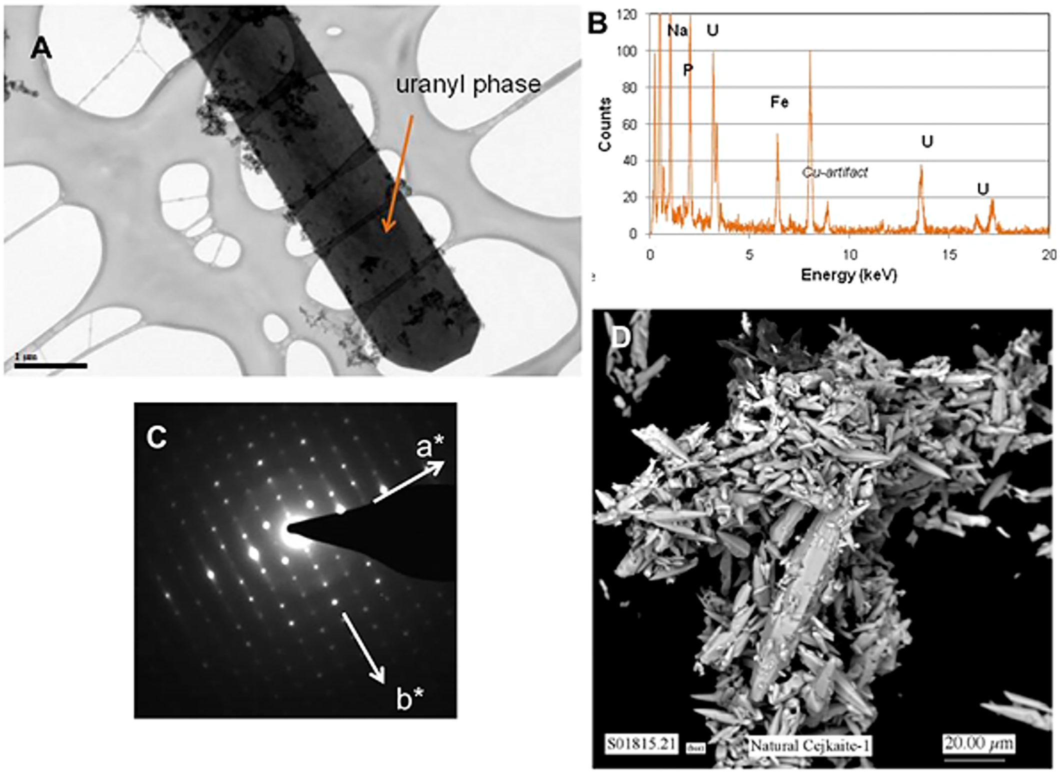

Figure 6. TEM image (a), EDS (b), and electron diffraction pattern of large uranyl phosphate grain (c).[47] SEM of cjerkite (d).[79]

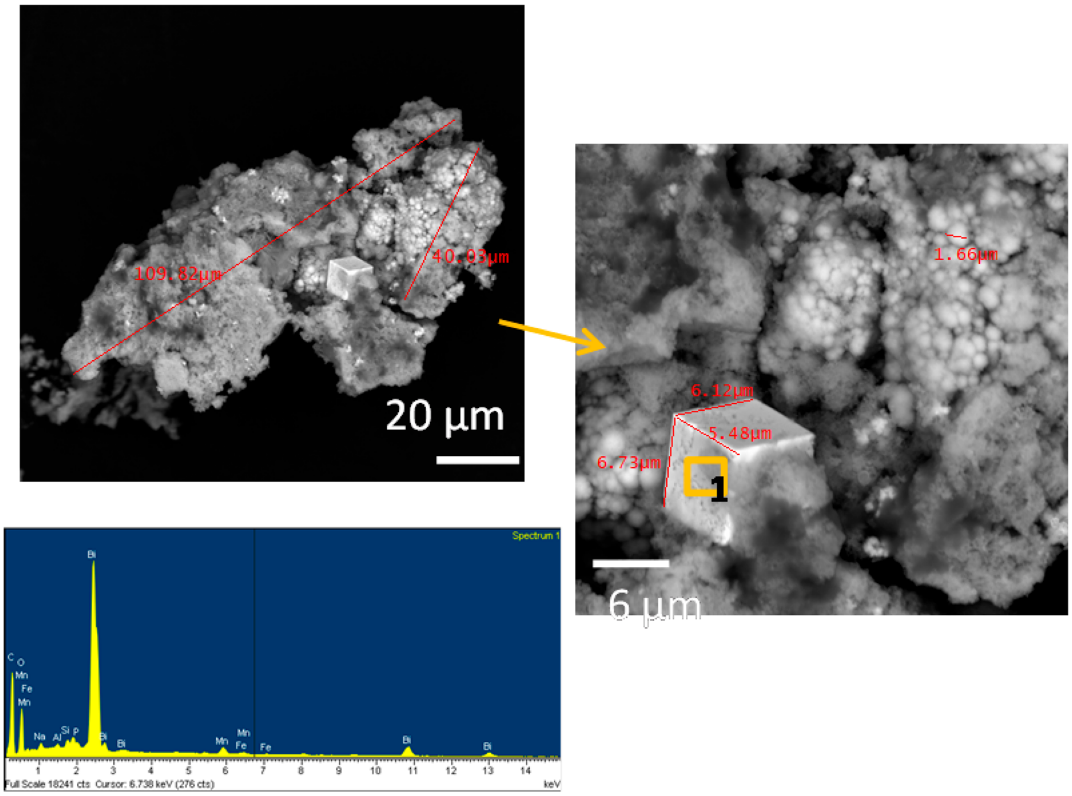

Figure 7. SEM images of an euhedral cubic Bi_2O_3 particle together with botryoidal bismuth phosphate agglomerates and EDS analysis (bottom panel) of the region within the yellow box (see right panel).[8]

particles could accumulate over time to cause a nuclear criticality event. More research is required to determine the potential impact of these particles on safety calculations for waste processing operations.

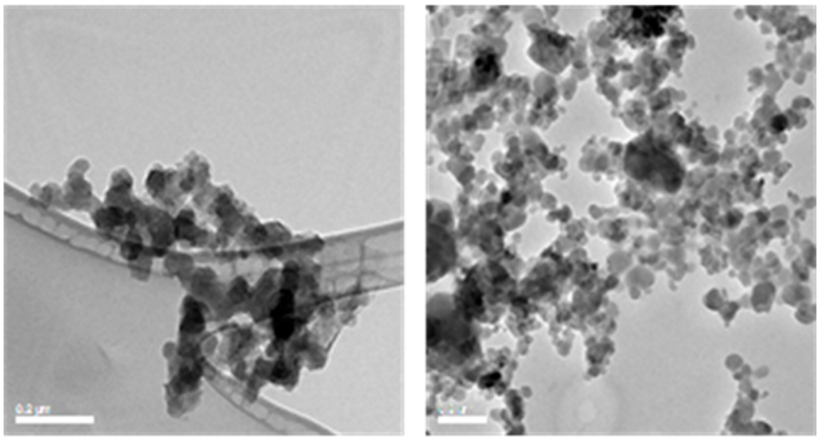

Figure 8. TEM images of BP sludge (left) and leached BP sludge that can be used for estimating the fractal dimension (right).[54]

During early Hanford operations, uranium was not recovered and became an appreciable waste component. Sodium uranate (Na_2UO_4) or the peroxide complex salt $Na_4UO_2(O_2)_3$ were predicted to precipitate in the tanks[76] and then alter to $U_3O_8 \cdot nH_2O$ and $UO_2 \cdot nH_2O$ at elevated temperatures (radioactivity generated heat) and the expected alkaline and anoxic conditions.[77] However, the paragenesis of U phases in the tanks has been complicated by a diversity of ligands. In the BiPP wastes, uranyl phosphate particles, several micrometers long and up to 1−2 μm across, formed (Figure 6, top).[47] The uranyl phosphates (see Lockock et al.[78] for details on crystallography) dissolve during caustic processing and reprecipitate as smaller amorphous particles.

The discovery by Krupka et al.[79] of the U carbonate phase cejkaite [$Na_4(UO_2)(CO_3)_3$] in C-203 and C-204 waste sludge had been predicted by Felmy et al.[80] (Figure 6, bottom right). The presence of cejkaite suggests that the tricarbonate complex ($UO_2(CO_3)_3{}^{4-}$) controls U solubility.[79,80] Other phases identified in this study, including goethite [α-FeOOH], maghemite (γ-Fe_2O_3), and clarkeite (and/or $Na_2U_2O_7$), have also been commonly observed in other sludge tank analyses. X-ray absorption near edge structure (XANES) revealed that uranyl(VI) phases dominate the uranium mineralogy in these sludge wastes.[81]

In addition to the uranyl phosphates discussed previously, bismuth oxide, bismuth phosphate, and a complex bismuth−iron silico-phosphate phase have also been identified in BiPP waste. The bismuth oxide phase occurs as plates or cubes, the bismuth phosphate as aggregates, and the silico-phosphate phase as a less distinct amorphous mass. La, Si, K, Cr, and Mn were also detected.[8] The complexity is illustrated in Figure 7, which shows a ∼5−7 μm euhedral cubic B_2O_3 particle embedded in a botryoidal bismuth phosphate agglomerate composed of much smaller particles. The bright white material is almost pure bismuth phosphate; however, the darker material also contains Si and Fe. There is a steady decrease in particle size and degree of obvious crystallinity going from bismuth oxide to bismuth phosphate to a mixed bismuth−iron silicate phosphate (see Table 1).

In contrast, other sludge samples, called bismuth-phosphate (BP) sludge, contain Bi−P phases but not bismuth oxide. Microanalysis of these samples[54] identified an iron bismuth phase, embedded in agglomerates (Figure 8, left), that is structurally related to bismuthoferrite [$BiFe^{3+}{}_2(SiO_4)_2(OH)$].[47] This phase was the most prominent particle in the sample and provides a better assessment of the agglomerate density, although additional characterization is necessary. Caustic leaching yielded particles with similar dimensions to the untreated bismuth-phosphate sludge (Figure 8, right), but were enriched in uranium and hence were denser.

The major aluminum phases include boehmite, gibbsite, as well as nitrate-cancrinite[82] and dawsonite.[83] The morphology of gibbsite crystals varies from thin, rounded hexagons and faceted lozenges to faceted plates and blocks with well-formed basal prismatic faces. Boehmite particles are considerably smaller than either gibbsite or dawsonite. When boehmite is present in excess of gibbsite, dispersion and reagglomeration processes "fluff-up" agglomerates; when gibbsite is in excess, the small boehmite particles attach to the larger particles and do not contribute to changing the density of the solids.

Boehmite crystallites expressed a rhombohedral platelet morphology, characteristic of formation at alkaline pH, and are only ∼30 nm thick with lateral dimensions that range from 30 to 350 nm (mode = 110 nm).[41] Note that stacking of boehmite crystals occurs in the [010] direction, which has implications for modeling the rheology but needs to be confirmed by cryo or in situ electron microscopy (Figure 9). Further, the round nanosize particles are uranium phases with trace Sr, and are very similar in dimension and appearance to the synthetic uranyl peroxide-nanoclusters examined by Soltis et al.[84] with cryo-TEM. Their close association with boehmite

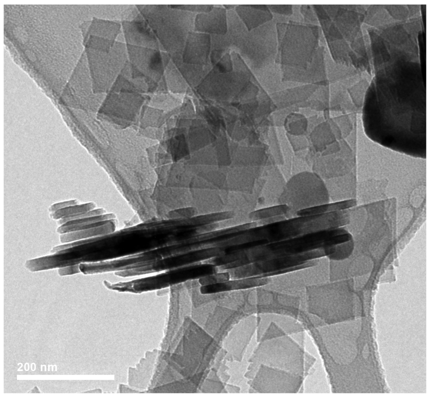

Figure 9. Bright field TEM image of boehmite REDOX sludge samples. Note that boehmite presents rhombohedral morphology and is stacked along the [010] direction. The round particles are uranium-rich (see text).

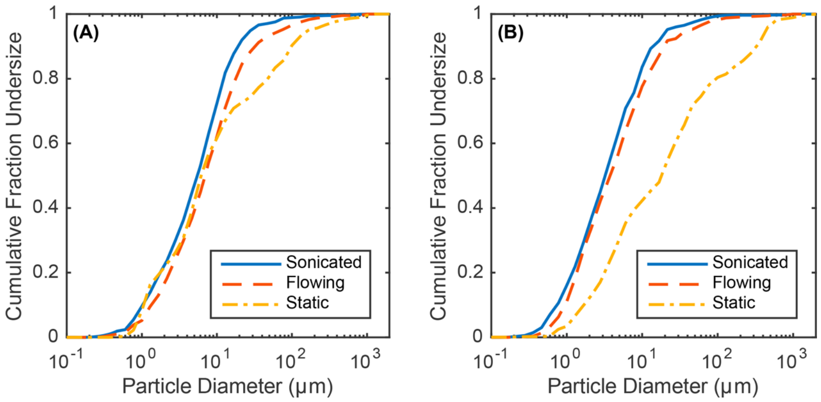

Figure 10. Representative PSDs for (A) sludge and (B) saltcake Hanford wastes under flowing sonicated ("sonicated"), flowing nonsonicated ("flowing"), and nonflowing ("static") conditions.

needs to be investigated as they might affect particle dynamics as well as signify U interaction with boehmite that may or may not influence thermodynamic/kinetic parameters that determine the extent and rate of boehmite caustic leaching.

Al and Cr are often closely associated, where the majority of the Al-material is amorphous.[3] TEM images (not shown) highlight the nanosized nature of the materials and their tendency to form agglomerates. TEM images (not shown) of caustic leached solid residue show the same basic morphology, although the leached phases are mostly devoid of aluminum and enriched in chromium.[3] In contrast, oxidative caustic leaching of Cr(III) solids to soluble Cr(VI) resulted in near complete release of Cr, but only a relatively small yet significant release of Al.[3] The exact relationship between Al and Cr, whether forming a solid solution or interdispersed Al- and Cr-rich nanoparticulates, has not been definitively determined, but the resolution of this issue is important for devising optimal leaching strategies for reducing the amount of Al during the waste treatment process.

Although there has been much progress in characterizing the sludge fraction using electron microscopy, it is evident that even higher spatial resolution is needed to tease apart elemental distributions and phase intergrowths. In this regard, the application of aberration-corrected TEM (ACTEM), which can attain subatomic resolution, to tank waste should push the science even further.

■ REPRESENTATIVE WASTE PARTICLE SIZE DISTRIBUTION

Knowledge of the PSD of both insoluble and soluble Hanford waste solids is needed to support design of systems that retrieve, transport, mix, and treat these wastes. Particle size measurements have been performed on numerous core and auger samples taken from the Hanford tanks as part of waste characterization, retrieval, safety, and pretreatment projects.[3,8,45,47,49−51,53,54,56,57,59,64,66,85−108] Despite the large body of work on waste PSD, not all tanks have been characterized, and many existing measurements are outdated due to transfers into tanks and/or chemical aging of the tank constituents. Furthermore, Hanford PSD measurements lack coherency due to the use of variable methodologies applied under different conditions.

Hanford PSD data indicate that solids range from the submicrometer up to approximately 1 mm and exist as individual primary particles and multicomponent particle agglomerates/flocculates with high variability among the tanks (see previous section). Recent compilations of historical Hanford PSD measurements have focused on laser diffraction measurements made under similar conditions.[8,53,67] For example, Wells et al.[8] report and developed representative PSDs for saltcake and sludge wastes under nonflowing and flowing conditions (±sonication); a subset is reproduced in Figure 10, which quantifies the effect of different flow regimes on the size of the aggregates. Such information is essential for developing and benchmarking physics-based models that predict waste rheology.

■ PROGRESS TOWARD NEXT GENERATION RESEARCH APPROACHES

Processing of the Hanford tank waste will take more than 40 years to complete. To date, this waste has been examined in an ex situ dried state, which may induce artifacts. Development of in situ and greater spatial/chemical resolution methods to examine highly radioactive samples will provide significant insight into the nature of HLW solids, and will potentially open up new cost saving processing options. Further, most modeling efforts have been phenomenological with limited scope and a primary focus on solution phase chemistry and equilibrium assessments of the solids phases that would form. However, development of a fundamental understanding of the interactions in complex metal hydroxide slurries will be essential for optimal operation of these facilities that are critical to the successful cleanup of one of the most complex environmental problems in the United States. A few examples are discussed where coupling of advanced characterization methods of these metal hydroxide slurries and theory can and are beginning to make progress toward a fundamental understanding of radioactive waste and waste-processing behavior at Hanford.

Tank waste slurries range from thin, water-like suspensions to thick pastes. These varying rheological properties drive significant design and operating considerations for waste treatment. To date, the particle properties that yield these widely varying slurry rheologies have not been identified. Slurry rheology depends on the coupling of hydrodynamics and particle−particle attractive/repulsive forces that act over different length and time scales, which in turn depend on solution characteristics and solid phase microstructure/hierarchical structures.[109,110] In this regard, physics-based predictive rheological correlations have been developed for simple cases (e.g., identical spherical particles).[111,112] The intrinsic complexity of Hanford waste slurries, however,

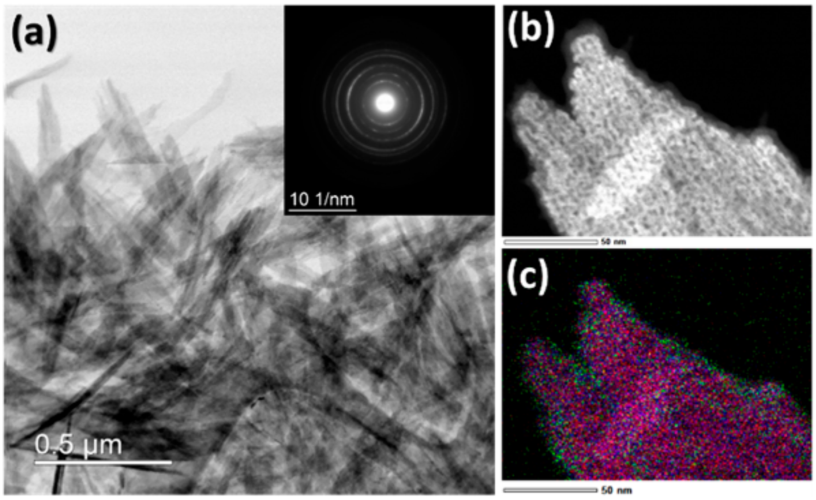

Figure 11. Microanalyses of Cr-doped boehmite: (a) TEM with selected-area electron diffraction inset, (b) STEM high-angle annular dark-field, and (c) energy-dispersive X-ray mapping of panel b (green spots represent Cr and purple spots represent Al). Reproduced from ref 124 with permission from The Royal Society of Chemistry.

prohibits extrapolating correlations from such simple systems. Indeed, Chun et al.[70] found that the Bingham-plastic yield stress of Hanford waste slurries was better correlated to the percentage of particles at less than about 5 μm rather than the median size. Consequently, tools need to be employed and developed for use with highly caustic radioactive materials to characterize the chemical physics at solid–liquid interfaces that determine interparticle forces as a function of irregular shape/surface topography, facet dependent surface charges/dielectric responses, and ion/solvent structures. An important development is the use of atomic force microscopy for measuring interactions between particles that can achieve force and distance resolutions of 1–100 pN and 0.5–2 nm, respectively.[113−115]

The application of in situ SEM/TEM for characterizing particle–particle interactions during static and flow conditions is another exciting development,[116] which if coupled to control of radiolysis products opens up opportunities to study the effect of radiation on aggregation and particle–particle interactions. Strong deviations from Derjaguin–Verwey–Overbeek–Landau (DLVO) theory are expected due, in part, to the high ionic strength of tank waste muting electrostatic interactions and increasing the contribution of van der Waals and other non-DLVO forces that operate at short-range. Consequently, the effect of water structures at solid–liquid interfaces on dispersion forces needs to be explicitly treated.[71] Further, recent improvements in computational schemes can be used to upscale microscopic observations to more complex macroscopic simulations.[117−121]

In addition to the need to understand particle–particle interactions, careful analyses of material size distributions and densities are required to assess such concerns as accumulation in pipelines during pumping operations and settling processes in tanks. An example of the need to switch from ex situ to in situ and cryo methods concerns the most common uranium phase in REDOX wastes: clarkeite.[41,90] Clarkeite is not only the most common uranium phase present, but it is also nominally the most dense uranium phase with implications for pumping operations. However, to estimate its effective density, one needs to use in situ or cryo-TEM to accurately characterize its morphology and particle–particle associations.

Another example of the need for advanced electron microscopy methods is given in Figure 9, where conventional TEM examination of uranium-rich particles (the round particles in Figure 9) reveals an atypical spherical morphology that could be an artifact of electron beam and/or drying/vacuum effects. For example, uranium peroxide nanoclusters,[122] are known to collapse and reduce to dense spherical U_3O_8 particles in the electron beam.[123] In contrast our own work[124] and numerous other studies have shown that boehmite is stabile (at least initially) under the electron beam during SEM and TEM analysis. Consequently, the spherical morphology of the uranium-rich particles might be an artifact and the original phase in the tanks could have a very different morphology and density. This further highlights the need for modern cryo-TEM and in situ TEM, as well as low-dose methods. In fact, using cryo methods would make it possible to explore for the occurrence of uranyl peroxide nanoclusters in the Hanford tanks and potentially provide definitive proof of radiation induced phase formation.

The dissolution rate of boehmite is the rate-limiting step in aluminum removal during chemical processing of wastes. Further, boehmite in tank waste dissolves 40 times more slowly than predicted given surface normalized rates.[41] Microanalysis of tank waste indicated a close association of Cr and Al, which inspired a recent experimental study on Cr(III)-boehmite interactions.[124] Detailed spectroscopy and microscopy of experimental samples, coupled to quantum mechanical theory, showed that Cr(III) did not substitute for Al(III) in the structure of boehmite regardless of synthesis route or particle morphology; rather, Cr was concentrated on edge surfaces, either as nano/micron size precipitates or as adsorbed complexes (Figure 11). Caustic leach tests indicated that Cr inhibited boehmite corrosion, possibly by pinning defects and blocking high energy surface sites. Consequently, a small concentration of Cr(III) could have a leveraged effect on boehmite dissolution. Further characterization of tank boehmite with ACTEM would more clearly define the relationship of Al and Cr, allowing for a more informed comparison with experiment.

As well as atomic resolution imaging of these materials, the ability to study chemical processes in situ promises greater insight into the interfacial chemistry and may enable new, innovative approaches to dealing with nuclear wastes. Recent work by Conroy et al.[125] has highlighted the use of liquid cell electron microscopy (LCEM) to probe the role of hydrogen bonding networks in stabilizing gibbsite and boehmite, two very important constituents of Hanford tank waste. This work was motivated by the very different dissolution behaviors of these two phases during processing. The primary result, based on real time observations, was that boehmite delaminated and dissolved whereas both gibbsite and Fe-doped boehmite were stable. The fact that dissolution and delamination were closely coupled, an observation made possible by using an in situ technique with high spatial resolution, provided strong evidence that differences in the hydrogen bond network holding the structural units of boehmite and gibbsite together was a key factor. That Fe-doped boehmite was stable points toward the importance of electron/hole recombination centers stabilizing the boehmite hydrogen bond network under radiation. Although the conditions in the LCEM were not the same as during processing (i.e., higher radiation and both lower pH and temperature), the fact that both gibbsite and Fe-doped (∼1%) boehmite were stable indicates that future LCEM experiments using these phases, but at higher pH and temperature, could reveal dissolution mechanisms under processing conditions without convoluting electron beam effects. However, this would involve developing more robust liquid cells that could withstand pH values and temperatures around 14 and 80 °C, respectively.

Significant characterization of Hanford tank waste was started 25 years ago. Design of the Hanford Tank Waste Treatment and Immobilization Plant began 17 years ago, in 2001. In the intervening years, there have been considerable improvements in the characterization tools available and in the ability to get radioactive waste samples into those instruments. The next generation tools that are beginning to be implemented, as outlined above, offer the ability to study tank waste solids in new and exciting ways, and offer the potential to illuminate new process schemes that would dramatically improve the performance of a key national endeavor; treatment of the Hanford waste that has been stored out in the desert of Washington State for nearly 70 years.

AUTHOR INFORMATION

Corresponding Author

*E-mail: reid.peterson@pnnl.gov.

ORCID

Eugene S. Ilton: 0000-0003-4931-5217

Gregg J. Lumetta: 0000-0002-0216-8515

Notes

The authors declare no competing financial interest.

ACKNOWLEDGMENTS

This work was supported by the Laboratory Directed Research and Development, Nuclear Processing Science Initiative. Pacific Northwest National Laboratory (PNNL) is a multiprogram national laboratory operated for the U.S. Department of Energy by Battelle Memorial Institute under Contract DE-AC06-76RLO 1830. A portion of this research was performed using the Environmental Molecular Sciences Laboratory, a national scientific user facility sponsored by the U.S. Department of Energy's Office of Biological and Environmental Research and located at the PNNL.

REFERENCES

(1) Gephart, R. E. *Hanford—A Conversation about Nuclear Waste and Cleanup*; Battelle Press: Richland, WA, 2003.

(2) Sylvester, P.; Rutherford, L. A.; Gonzalez-Martin, A.; Kim, J.; Rapko, B. M.; Lumetta, G. J. Ferrate treatment for removing chromium from high-level radioactive tank waste. *Environ. Sci. Technol.* **2001**, *35* (1), 216−221.

(3) Fiskum, S. K.; Buck, E. C.; Daniel, R. C.; Draper, A. E.; Edwards, M. K.; Hubler, T. L.; Jagoda, L. K.; Jenson, E. D.; Kozelisky, A. E.; Lumetta, G. J.; MacFarlan, P. J.; McNamara, B. K.; Peterson, R. A.; Sinkov, S. I.; Snow, L. A.; Swoboda, M. P. *Characterization and Leach Testing for REDOX Sludge and S-Saltcake Actual Waste Sample Composites*; PNNL-17368; Pacific Northwest National Laboratory: Richland, WA, 2008; http://www.pnl.gov/main/publications/external/technical_reports/PNNL-17368.pdf.

(4) Best Basis Inventory. https://twins.labworks.org/twinsdata/Forms/About.aspx?subject=BestBasisInventory.

(5) Higley, B. A.; Place, D. E. *Hanford Defined Waste Model*, Revision 5.0, RPP-19822, Rev. 0; CH2M Hill Hanford Group: Richland, WA, 2004; http://pdw.hanford.gov/arpir/index.cfm/viewDoc?accession=0081017H.

(6) Klem, M. J. *Inventory of Chemicals Used at Hanford Production Plants and Support Operations (1944−1980)*, Rev.1, WHC-EP-0172; Westinghouse Hanford Company: Richland, WA, 1990; https://www.osti.gov/scitech/servlets/purl/7046574.

(7) Hanford Federal Facility Agreement and Consent Order. http://www.hanford.gov/page.cfm/TriParty/TheAgreement.

(8) Wells, B. E.; Kurath, D. E.; MaHoney, L. A.; Onishi, Y.; Huckaby, J. L.; Cooley, S. K.; Burns, C. A.; Buck, E. C.; Tingey, J. M.; Daniel, R. C.; Anderson, K. K. *Hanford Waste Physical and Rheological Properties: Data and Gaps*, PNNL-20646; Pacific Northwest National Laboratory: Richland, WA, 2011; http://www.pnnl.gov/main/publications/external/technical_reports/PNNL-20646.pdf.

(9) Cooke, G. A.; Pestovich, J. A. *C-104 Solid Phase Characterization of Sample 4C-13−1 from Tank 241-C-104 Closure Sampling Event*, LAB-RPT-13−00005 RO; Washington River Protection Solutions LLC: Richland, WA, 2013; https://www.osti.gov/scitech/servlets/purl/1083295/.

(10) Cleveland, J. M. *The Chemistry of Plutonium*; Gordon and Breach Science Publishers: New York, 1970.

(11) Hanford Engineer Works technical manual, Section C—Separations, HW-10475. http://www.osti.gov/scitech/biblio/6892962-hanford-engineer-works-technical-manual.

(12) Clark, D. L.; Hecker, S. S.; Jarvinen, G. D.; Neu, M. P. *Plutonium*, 3rd ed.; Springer: Dordrecht, The Netherlands, 2006; Chapter 7, p 841.

(13) Cleveland, J. M. Chapter 14. In *Plutonium Handbook: A Guide to the Technology*, Wick, O. J., Ed. Gordon and Breach: New York, 1967; Vol. *II*.

(14) Swanson, J. L. PUREX Process Flowsheets. In *Science and Technology of Tributyl Phosphate*; CRC Press: Boca Raton, FL, 1990; pp 55−79.

(15) Swanson, J. L. The Zirflex Process. In *Process Chemistry*; Pergamon: Oxford, 1961; pp 289−303.

(16) *Uranium Recovery Technical Manual*, HW-19140-DEL; Hanford Works: Richland, WA, 1951; https://www.ntis.gov/Search/Home/titleDetail/?abbr=HW19140DEL.

(17) Runion, T. C.; Ellison, C. V. *TBP Process for Uranium Recovery from Metal Waste—Laboratory Studies*; ORNL-557; Oak Ridge National Laboratory: Oak Ridge, TN, 1950; https://www.osti.gov/scitech/servlets/purl/4177852.

(18) Salem, R.; Lewandowski, R.; Roberts, C.; Goin, J.; Thurston, K.; Abouljoud, M.; Courtney, A. Use of yttrium-90 glass microspheres (TheraSphere) for the treatment of unresectable hepatocellular carcinoma in patients with portal vein thrombosis. *Journal of Vascular and Interventional Radiology* **2004**, *15* (4), 335−345.

(19) Coldwell, D. M.; Kennedy, A. S.; Nutting, C. W. Use of yttrium-90 microspheres in the treatment of unresectable hepatic metastases

from breast cancer. *Int. J. Radiat. Oncol., Biol., Phys.* **2007**, *69* (3), 800−804.

(20) Inarrairaegui, M.; Thurston, K. G.; Bilbao, J. I.; D'Avola, D.; Rodriguez, M.; Arbizu, J.; Martinez-Cuesta, A.; Sangro, B. Radioembolization with Use of Yttrium-90 Resin Microspheres in Patients with Hepatocellular Carcinoma and Portal Vein Thrombosis. *Journal of Vascular and Interventional Radiology* **2010**, *21* (8), 1205−1212.

(21) Osterholm, M. T.; Norgan, A. P. The role of irradiation in food safety. *N. Engl. J. Med.* **2004**, *350* (18), 1898−1901.

(22) Schulz, W. W.; Bray, L. A. Solvent-Extraction Recovery of By-product CS-137 and SR-90 from HNO_3 Solutions - A Technology Review and Assessment. *Sep. Sci. Technol.* **1987**, *22* (2−3), 191−214.

(23) Burns, R. E.; Stedwell, M. J. Volume reduction of radioactive waste by carrier precipitation. *Chemical Engineery Progress* **1957**, *53* (2), 93−95.

(24) Cash, R. J.; Meacham, J. E.; Lilga, M. A.; Babad, H. *Resolution of the Hanford Site Ferrocyanide Safety Issue*, HNF-SA-3126-FP; DE&S Hanford Inc.: Richland, WA, 1997; http://pdw.hanford.gov/arpir/pdf.cfm?accession=0071666H.

(25) Barton, W. B.; Gale, L. A.; Johnson, M. E. In *Sixteen Years of Cesium Recovery Processing at Hanford's B Plant, RHO-RE-SA-169, Rockwell Hanford Operations, Richland, WA*, American Nuclear Society International, Spectrum 86: Niagara Falls, NY, 1986.

(26) Schulz, W. W.; Richardson, G. L.; Mendel, J. E. Solvent Extraction Recovery and Purification of Strontium-90. *Ind. Eng. Chem. Process Des. Dev.* **1963**, *2* (2), 134−140.

(27) *Waste Management Technical Manual*, ISO-100; Isochem, Inc.: Richland, WA, 1967; https://www.osti.gov/scitech/biblio/10180948.

(28) Reynolds, J. G.; Reynolds, D. A. *A Modern Interpretation of the Barney Diagram for Aluminum Solubility in Tank Waste*, WRPS-44083-FP; Washington River Protection Solutions: Richland, WA, 2009; https://www.osti.gov/scitech/servlets/purl/969692.

(29) Reynolds, J. G.; Herting, D. L. *Solubilities of Sodium Nitrate, Sodium Nitrite and Sodium Aluminate in Simulated Nuclear Waste*; Rockwell Hanford Operations: Richland, WA, 1984; www.iaea.org/inis/collection/NCLCollectionStore/_Public/16/035/16035295.pdf.

(30) Toghiani, R. K.; Phillips, V. A.; Lindner, J. S. Solubility of Na-F-SO4 in water and in sodium hydroxide solutions. *J. Chem. Eng. Data* **2005**, *50* (5), 1616−1619.

(31) Toghiani, R. K.; Phillips, V. A.; Smith, L. T.; Lindner, J. S. Solubility in the Na+SO4+NO3 and Na+SO4+NO2 systems in water and in sodium hydroxide solutions. *J. Chem. Eng. Data* **2008**, *53* (3), 798−804.

(32) Felmy, A. R. *Thermodynamic Modeling of Sr/TRU Removal*; Bechtel National, Inc.: Richland, WA, 2000; www.pnl.gov/rpp-wtp/documents/BNFL-RPT-037.PDF.

(33) Felmy, A. R.; MacLean, G. T. *Development of an Enhanced Thermodynamic Database for the Pitzer Model in ESP: The Fluoride and Phosphate Components*; Bechtel National, Inc.: Richland, WA, 2001; www.pnl.gov/rpp-wtp/documents/WTP-RPT-018.pdf.

(34) Felmy, A. R.; MacLean, G. T. *Thermodynamic Modeling of AZ-101 Slurry Leaching*, PNWD-3289, WTP-RPT-067, Rev 0, Final Report; Prepared for Bechtel National Inc. by Battelle-Pacific Northwest Division: Richland, WA, 2002; http://www.pnl.gov/rpp-wtp/documents/WTP-RPT-067.pdf.

(35) Felmy, A. R.; Mason, M. J.; Qafoku, O. S. *Thermodynamic Data Development for Modeling Sr/TRU Separations: Sr-EDTA, Sr-HEDTA, and Mn-Gluconate Complexation*, WTP-RPT-083; Prepared for Bechtel National Inc. by Battelle Pacific Northwest Division: Richland, WA, 2004; http://www.pnl.gov/rpp-wtp/documents/WTP-RPT-083.pdf.

(36) Rapko, B. M.; Blanchard, D. L.; Colton, N. G.; Felmy, A. R.; Liu, J.; Lumetta, G. J. *The Chemistry of Sludge Washing and Caustic Leaching Processes for Selected Hanford Tank Wastes*, PNNL-11089; Pacific Northwest National Laboratory: Richland, WA, 1996; https://www.osti.gov/scitech/servlets/purl/219403.

(37) Rapko, B. M.; Burgeson, I. E.; Cho, H.; Deschane, J.; Felmy, A. R.; Jenson, E.; McNamara, B. K.; Poloski, A. P.; Snow, L.; MacLean, G. T. *Mixing of WTP Process Solutions*, WTP-RPT-080, Rev 0; Prepared for Bechtel National Inc. by Battelle Pacific Northwest Division: Richland, WA, 2003; http://www.pnl.gov/rpp-wtp/documents/WTP-RPT-080.pdf.

(38) Reynolds, J. G.; Carter, R. Pitzer Model Anion-Anion and Ternary Interaction Parameters for the Na2C2O4-NaOH-H2O and Na2C2O4-NaNO3-H2O Systems. *J. Solution Chem.* **2015**, *44* (7), 1358−1366.

(39) Reynolds, J. G.; Carter, R. A sulfate and darapskite solubility model with Pitzer interaction coefficients for aqueous solutions containing $NaNO_2$, $NaNO_3$, and NaOH. *J. Chem. Thermodyn.* **2016**, *101*, 380−386.

(40) Reynolds, J. G.; Carter, R.; Felmy, A. R. A Pitzer Interaction Model for the NaNO3-$NaNO_2$-NaOH-H_2O System from 0 to 100 degrees C. *Ind. Eng. Chem. Res.* **2015**, *54* (11), 3062−3070.

(41) Snow, L. A.; Lumetta, G. J.; Fiskum, S.; Peterson, R. A. Boehmite actual waste dissolution studies. *Sep. Sci. Technol.* **2008**, *43* (9−10), 2900−2916.

(42) Amato, L. C.; Nuttall, G. L.; Johnson, K. W.; Lambie, R. W.; DiCenso, A. T.; Schreiber, R. D.; Simpson, B. C. *Tank Characterization Report for Single-Shell Tank 241-C-110*, WHC-SD-WM-ER-367; Westinghouse Hanford Company: Richland, WA, 1994; https://www.osti.gov/scitech/servlets/purl/10185383.

(43) Baldwin, D. L.; Bredt, P. R.; Campbell, J. A.; Farmer, O. T.; Fiskum, S. K.; Greenwood, L. R.; Mong, G. M.; Poloski, A. P.; Scheele, R. D.; Soderquist, C. V.; Smith, M. R.; Snow, L. A.; Swoboda, M. P.; Thomas, M. P.; Urie, M. W.; Wagner, J. J. *Chemical Analysis and Physical Property Testing of 241-AP-104 Tank Waste*, WTP-RPT-069, Rev. 0 (PNWD-3334); Pacific Northwest National Laboratory: Richland, WA, 2003; http://www.pnl.gov/rpp-wtp/.

(44) Baldwin, D. L. *Tank Characterization Report for Single-Shell Tank 241-T-102*, HNF-SD- WM-ER-700, Rev. 0; Fluor Daniel Hanford, Inc.: Richland, WA, 1997; http://www.iaea.org/inis/collection/NCLCollectionStore/_Public/30/035/30035853.pdf.

(45) Brooks, K. P.; Bredt, P. R.; Golcar, G. R.; Hartley, S. A.; Jagoda, L. K.; Rappe, K. G.; Urie, M. W. *Characterization, Washing, Leaching, and Filtration of C-104 Sludge*, BNFL-RPT-030; Battelle Pacific Northwest Division: Richland, WA, 2000; https://www.osti.gov/scitech/servlets/purl/756361.

(46) Coleman, C. J. *Compositing and Characterization of Samples from Hanford Tank 241-AY-102/C-106*; WSRC-TR-2003−00205; Westinghouse Savannah River Company: Aiken, SC, 2004; http://sti.srs.gov/fulltext/tr2003205/tr2003205.pdf.

(47) Edwards, M. K.; Billings, J. M.; Blanchard, D. L.; Buck, E. C.; Casella, A. J.; Casella, A. M.; Crum, J. V.; Daniel, R. C.; Draper, A. E.; Fiskum, S. K.; Jagoda, L. K.; Jenson, E. D.; Kozelisky, A. E.; MacFarlan, P. J.; Peterson, R. A.; Shimsky, R. W.; Snow, L. A.; Swoboda, M. P. *Characterization, Leaching, and Filtration Testing for Tributyl Phosphate (TBP, Group 7) Actual Waste Sample Composites*, PNNL-18119; Pacific Northwest National Laboratory: Richland, WA, 2009; http://www.pnl.gov/main/publications/external/technical_reports/PNNL-18119.pdf.

(48) DiCenso, A. T.; Amato, L. C.; Lambie, R. W.; Franklin, J. D.; Seymour, B. J.; Johnson, K. W.; Stevens, R. H.; Remund, K. M.; Sasaki, L. M.; Simpson, B. C. *Tank Characterization Report for Single-Shell Tank 241-C-109*, WHC-SD-WM-ER-402; Westinghouse Hanford Company: Richland, WA, 1995; http://www.iaea.org/inis/collection/NCLCollectionStore/_Public/26/060/26060610.pdf.

(49) Fiskum, S. K.; Billings, J. M.; Crum, J. V.; Daniel, R. C.; Edwards, M. K.; Shimsky, R. W.; Peterson, R. A.; MacFarlan, P. J.; Buck, E. C.; Draper, A. E.; Kozelisky, A. E. *Characterization, Leaching, and Filtrations Testing of Ferrocyanide Tank Sludge (Group 8) Actual Waste Composite*, PNNL-18120; Pacific Northwest National Laboratory: Richland, WA, 2009; www.pnl.gov/main/publications/external/technical_reports/PNNL-18120.pdf.

(50) Geeting, J. G. H.; Hallen, R. T. Filtration, washing, and caustic leaching of Hanford Tank AZ-101 sludge. *Sep. Sci. Technol.* **2005**, *40*, 1−15.

(51) Herting, D. L. *Results of Dilution Studies with Waste from Tank 241-AN-104*, HNF-3352, Rev. 0; Fluor Daniel Hanford, Inc.: Richland, WA, 1998; https://www.osti.gov/scitech/servlets/purl/782273.

(52) Herting, D. L. *Tank 241-S-112 Saltcake Dissolution Laboratory Test Report*, RPP-10984, Rev. 0; Fluor Hanford Inc.: Richland, WA, 2002; http://rkc.pnl.gov/docs/files/webviewable-RPP-10984,%20Rev.0.pdf.

(53) Wells, B. E.; Knight, M. A.; Buck, E. C.; Daniel, R. C.; Cooley, S. K.; MaHoney, L. E.; Meyer, P. A.; Poloski, A. P.; Tingey, J. M.; Callaway, W. S.; Cooke, G. A.; Johnson, K. W.; Thien, M. G.; Washenfelder, D. J.; Davis, J. J.; Hall, M. N.; Smith, G. L.; Thomson, S. L.; Onishi, Y. *Estimate of Hanford Waste Insoluble Solid Particle Size And Density Distribution*, PNWD-3824; Battelle-Pacific Northwest Division: Richland, WA, 2007; http://www.pnl.gov/rpp-wtp/documents/WTP-RPT-153.pdf.

(54) Lumetta, G. J.; Buck, E. C.; Daniel, R. C.; Draper, A. E.; Edwards, M. K.; Fiskum, S. K.; Hallen, R. T.; Jagoda, L. K.; Jenson, E. D.; Kozelisky, A. E.; MacFarlan, P. J.; Peterson, R. A.; Shimsky, R. W.; Sinkov, S. I.; Snow, L. A. *Characterization, Leaching, and Filtration Testing for Bismuth Phosphate Sludge (Group 1) and Bismuth Phosphate Saltcake (Group 2) Actual Waste Sample Composites*, PNNL-17992; Pacific Northwest National Laboratory: Richland, WA, 2009; http://www.pnl.gov/main/publications/external/technical_reports/PNNL-17992.pdf.

(55) Martin, K. B. *Compositing, Homogenization, and Characterization of Samples from Hanford Tank 241-AN-107*, WSRC-TR-2003−00210, Rev. 0; Westinghouse Savannah River Company: Aiken, SC, 2004; http://sti.srs.gov/fulltext/tr2003210/tr2003210.pdf.

(56) Onishi, Y.; Shekarriz, R.; Recknagel, K. P.; Smith, P. A.; Liu, J.; Chen, Y. L.; Rector, D. R.; Hudson, D. J. *Tank SY-102 Waste Retrieval Assessment: Rheological Measurements and Pump Jet Mixing Simulations*, PNNL-11352; Pacific Northwest National Laboratory: Richland, WA, 1996; https://www.osti.gov/scitech/servlets/purl/416963.

(57) O'Rourke, J. F. *Results of Retrieval Studies with Waste from Tank 241-C-104*, RPP-5798, Rev. 0; Fluor Hanford Inc.: Richland, WA, 2000; http://rkc.pnl.gov/docs/files/webviewable-RPP-5798,%20Rev.0.pdf.

(58) Poirier, M. R. *Filtration of a Hanford AN-104 Sample*, WSRC-TR-2003−00295, Rev. 0; Westinghouse Savannah River Company: Aiken, SC, 2003; http://sti.srs.gov/fulltext/tr2003295/tr2003295.pdf.

(59) Raphael, G. F. *Tank Characterization Report for Single-Shell Tank 241-BX-107*, WHC-EP-0739; Westinghouse Hanford Company: Richland, WA, 1994; http://www.iaea.org/inis/collection/NCLCollectionStore/_Public/26/034/26034286.pdf.

(60) Rasmussen, J. H. *Tank Characterization Report for Single-Shell Tank 241-B-202*, WHC-SD-WM-ER-371, Rev. 0-C; Lockheed Martin Hanford Corp.: Richland, WA, 1999; http://pdw.hanford.gov/arpir/pdf.cfm?accession=D199110707.

(61) Rassat, S. D.; MaHoney, L. E.; Wells, B. E.; Mendoza, D. P.; Caldwell, D. D. *Assessment of Physical Properties of Transuranic Waste In Hanford Single-Shell Tanks*, PNNL-14221; Pacific Northwest National Laboratory: Richland, WA, 2003; http://www.pnl.gov/main/publications/external/technical_reports/PNNL-14221.pdf.

(62) Reynolds, D. A. *Tank 101-SY Window E Core Sample: Interpretation of Results*, WHC-EP-0628; Westinghouse Hanford Company: Richland, WA, 1993; http://www.iaea.org/inis/collection/NCLCollectionStore/_Public/24/070/24070374.pdf.

(63) Simpson, B. C.; Borsheim, G. L.; Jenson, L. *Tank Characterization Report: Tank 241-C-112*, WHC-EP-0640, Rev. 1; Westinghouse Hanford Company: Richland, WA, 1993; http://rkc.pnl.gov/docs/files/webviewable-WHC-EP--0640.pdf.

(64) Snow, L. A.; Buck, E. C.; Casella, A. J.; Crum, J. V.; Daniel, R. C.; Draper, A. E.; Edwards, M. K.; Fiskum, S. K.; Jagoda, L. K.; Jenson, E. D.; Kozelisky, A. E.; MacFarlan, P. J.; Peterson, R. A.; Swoboda, M. P. *Characterization and Leach Testing for Purex Cladding Waste Sludge (Group 3) and Redox Cladding Waste Sludge (Group 4) Actual Waste Sample Composites*, PNNL-18054; Pacific Northwest National Laboratory: Richland, WA, 2009.

(65) Tingey, J. M.; Gao, J.; Delegard, C. H.; Bagaasen, L. M.; Wells, B. E. *Physical Property and Rheological Testing of Actual Transuranic Waste from Hanford Single-Shell Tanks*, PNNL-14365; Pacific Northwest National Laboratory: Richland, WA, 2003; http://www.pnl.gov/main/publications/external/technical_reports/PNNL-14365.pdf.

(66) Urie, M. W.; Bredt, P. R.; Caldwell, D. D.; Farmer, O. T.; Greenwood, L. R.; Jagoda, L. K.; Mong, G. M.; Poloski, A. P.; Reed, L. L.; Scheele, R. D.; Soderquist, C. V.; Swoboda, M. P.; Thomas, M. P.; Wagner, J. J. *Chemical and Physical Properties Testing of 241-AN-102 Tank Waste Blended with 241-C-104 Wash/Leachate Solutions*, WTP-RPT-021, Rev. 1 (PNWD-3228); Battelle-Pacific Northwest Division: Richland, WA, 2002; http://www.pnl.gov/rpp-wtp/.

(67) Meacham, J. E.; Harrington, S. J.; Rodriquez, J. S.; Nguyen, V. C.; Reynolds, J. D.; Wells, B. E.; Piepel, G. F.; Cooley, S. K.; Enderlin, C. W.; Rector, D. R.; Chun, J.; Heredia-Langner, A.; Gimpel, R. F. *One System Evaluation of Waste Transferred to the Waste Treatment Plant*, RPP-RPT-51652, Rev. 0, (PNNL-21410, Rev. 0); Washington River Protection Solutions LLC: Richland, WA, 2012.

(68) Herting, D. L.; Cooke, G. A. *Identification of Solid Phases in Saltcake from Hanford Site Waste Tanks*, HNF-11585, Rev.0; Fluor Hanford, Inc.: Richland, WA, 2002; https://www.osti.gov/scitech/servlets/purl/808264.

(69) Lumetta, G. J.; Rapko, B. M.; Cho, H. M. Studies of the Fundamental Chemistry of Hanford Tank Sludges. *ASME 2003 9th International Conference on Radioactive Waste Management and Environmental Remediation* **2003**, 177−184.

(70) Chun, J.; Oh, T.; Luna, M.; Schweiger, M. Effect of particle size distribution on slurry rheology: Nuclear waste simulant slurries. *Colloids Surf., A* **2011**, *384* (1−3), 304−310.

(71) Chun, J. H.; Mundy, C. J.; Schenter, G. K. The Role of Solvent Heterogeneity in Determining the Dispersion Interaction between Nanoassemblies. *J. Phys. Chem. B* **2015**, *119* (18), 5873−5881.

(72) Prakash, A.; Pfaendtner, J.; Chun, J. H.; Mundy, C. J. Quantifying the Molecular-Scale Aqueous Response to the Mica Surface. *J. Phys. Chem. C* **2017**, *121* (34), 18496−18504.

(73) Reynolds, J. G.; Page, J. S.; Cooke, G. A.; Pestovich, J. A scanning electron microscopy study of bismuth and phosphate phases in bismuth phosphate process waste at Hanford. *J. Radioanal. Nucl. Chem.* **2015**, *304* (3), 1253−1259.

(74) Reynolds, J. G.; Cooke, G. A.; McCoskey, J. K.; Callaway, W. S. Discovery of plutonium-bismuth and plutonium-bismuth-phosphorus containing phases in a Hanford waste tank. *J. Radioanal. Nucl. Chem.* **2016**, *309* (3), 973−981.

(75) Bell, J. T.; Bell, L. H. Separations Technology: The Key to Radioactive Waste Minimization. In *Chemical Pretreatment of Nuclear Waste for Disposal*; Schulz, W. W., Horwitz, E. P., Eds.; Plenum Press: New York, 1994.

(76) Krot, N. N.; Shilov, V. P.; Feodseev, A. M.; Yussov, A. B.; Bessonov, A. A.; Budantseva, N. A.; Nikitenko, S. I.; Plavnik, G. M.; Puraeva, T. P.; Grigoriev, M. S.; Garnov, A. Y.; Gelis, A. V.; Perminov, V. P.; Astafurova, L. N.; Delegard, C. H. *Alkaline Treatment of Acidic Solution from Hanford K Basin Sludge Dissolution*, PNNL 11944; Pacific Northwest National Laboratory: Richland, WA, 1998; https://digital.library.unt.edu/ark:/67531/metadc672107/.

(77) Giammar, D. E.; Hering, J. G. Influence of dissolved sodium and cesium on uranyl oxide hydrate solubility. *Environ. Sci. Technol.* **2004**, *38* (1), 171−179.

(78) Locock, A. J.; Burns, P. C.; Duke, M. J. M.; Flynn, T. M. Monovalent cations in structures of the meta-autunite group. *Can. Mineral.* **2004**, *42*, 973−996.

(79) Krupka, K. M.; Schaef, H. T.; Arey, B. W.; Heald, S. M.; Deutsch, W. J.; Lindberg, M. J.; Cantrell, K. J. Residual waste from Hanford tanks 241-C-203 and 241-C-204. 1. Solids characterization. *Environ. Sci. Technol.* **2006**, *40* (12), 3749−3754.

(80) Felmy, A. R.; Xia, Y. X.; Wang, Z. M. The solubility product of NaUO2PO4 center dot xH(2)O determined in phosphate and carbonate solutions. *Radiochim. Acta* **2005**, *93* (7), 401−408.

(81) Krupka, K. M.; Cantrell, K. J.; Schaef, H. T.; Arey, B. W.; Heald, S. M.; Deutsch, W. J.; Lindberg, M. J. Characterizing Solids in Residual Wastes from Single-Shell Tanks at the Hanford Site. *Radwaste Solutions* **2010**, *17* (2), 64−75.

DOI: 10.1021/acs.est.7b04077
Environ. Sci. Technol. 2018, 52, 381−396

(82) Buck, E. C.; McNamara, B. K. Precipitation of nitrate - Cancrinite in Hanford tank sludge. *Environ. Sci. Technol.* **2004**, *38* (16), 4432−4438.

(83) Reynolds, J. G.; Cooke, G. A.; Herting, D. L.; Warrant, R. W. Evidence for Dawsonite in Hanford high-level nuclear waste tanks. *J. Hazard. Mater.* **2012**, *209-210*, 186−192.

(84) Soltis, J. A.; Wallace, C. M.; Penn, R. L.; Burns, P. C. Cation-Dependent Hierarchical Assembly of U60 Nanoclusters into Macro-Ion Assemblies Imaged via Cryogenic Transmission Electron Microscopy. *J. Am. Chem. Soc.* **2016**, *138* (1), 191−198.

(85) Beck, M. A. *Analysis Report for 241-BY-104 Auger Samples*, WHC-SD-WM-TI-540, Rev. 1; Westinghouse Hanford Company: Richland, WA, 1994; http://www.iaea.org/inis/collection/NCLCollectionStore/_Public/26/038/26038240.pdf?.

(86) Brooks, K. P.; Bontha, J. R.; Golcar, G. R.; Myers, R. L.; Rappe, K. G.; Rector, D. R. *Bench-Scale Enhanced Sludge Washing and Gravity Settling Of Hanford Tank S-107 Sludge*, PNNL-12010; Pacific Northwest National Laboratory: Richland, WA, 1998; http://www.pnl.gov/main/publications/external/technical_reports/PNNL-12010.pdf.

(87) Brooks, K. P.; Bredt, P. R.; Cooley, S. K.; Golcar, G. R.; Jagoda, L. K.; Rappe, K. G.; Urie, M. W. *Characterization, Washing, Leaching, and Filtration of AZ-102*, PNWD-3045, BNFL-RPT-038; Battelle-Pacific Northwest Division: Richland, WA, 2000; https://www.osti.gov/scitech/servlets/purl/760429.

(88) Buck, E. C.; Arey, B. W.; Fiskum, S. K.; Geeting, J. G. H.; Jenson, E. D.; McNamara, B. K.; Poloski, A. P. *Characterization of Hanford Tanks 241-AN-102 and AZ-101 Washed Solids with X-Ray Diffraction, Scanning Electron Microscopy, and Light-Scattering Particle Analysis*, WTP-RPT-076 (PNWD-3300); Battelle-Pacific Northwest Division: Richland, WA, 2003; http://www.pnl.gov/rpp-wtp/.

(89) DiCenso, A. T.; Amato, L. C.; Franklin, J. D. N. G.L.; Johnson, K. W.; Sathyanarayana, P.; Simpson, B. C. *Tank Characterization Report for Single-Shell Tank 241-S-104*, WHC-SD-WM-ER-370; Westinghouse Hanford Company: Richland, WA, 1994; https://www.osti.gov/scitech/servlets/purl/10189762.

(90) Lumetta, G. J.; Burgeson, I. E.; Wagner, J. J.; Liu, J.; Chen, Y. L. *Washing and Caustic Leaching of Hanford Tank Sludge: Results of FY 1997 Studies*, PNNL-11636; Pacific Northwest National Laboratory: Richland, WA, 1997; http://www.iaea.org/inis/collection/NCLCollectionStore/_Public/29/039/29039286.pdf.

(91) Lumetta, G. J.; Rapko, B. M. *Washing and Alkaline Leaching of Hanford Tank Sludges: A Status Report*, PNNL-10078; Pacific Northwest National Laboratory: Richland, WA, 1994; https://www.osti.gov/scitech/servlets/purl/10181387.

(92) Lumetta, G. J.; Rapko, B. M.; Wagner, J. J.; Liu, J.; Chen, Y. L. *Washing and Caustic Leaching of Hanford Tank Sludges: Results of FY 1996 Studies*, PNNL-11278; Pacific Northwest National Laboratory: Richland, WA, 1996; https://www.iaea.org/inis/collection/NCLCollectionStore/_Public/28/014/28014630.pdf.

(93) Lumetta, G. J.; Wagner, J. J.; Hoopes, F. V.; Steele, R. T. *Washing and Caustic Leaching of Hanford Tank C-106 Sludge*, PNNL-11381; Pacific Northwest National Laboratory: Richland, WA, 1996; https://www.osti.gov/scitech/servlets/purl/416962.

(94) Morrey, E. V.; Tingey, J. M. *Comparison of Simulants to Actual Neutralized Current Acid Waste: Process and Product Testing Of Three NCAW Core Samples from Tanks 101-AZ and 102-AZ*, PNNL-11098; Pacific Northwest National Laboratory: Richland, WA, 1996; http://www.iaea.org/inis/collection/NCLCollectionStore/_Public/27/063/27063373.pdf.

(95) Morrey, E. V.; Tingey, J. M.; Elliott, M. L. *Comparison of Simulants to Actual Neutralized Current Acid Waste: Process and Product Testing of Three NCAW Core Samples from Tanks 101-AZ and 102-AZ*, PNNL-11025; Pacific Northwest National Laboratory: Richland, WA, 1996; http://www.iaea.org/inis/collection/NCLCollectionStore/_Public/28/022/28022138.pdf.

(96) Peterson, M. E.; Scheele, R. D.; Tingey, J. M. *Characterization of the First Core Sample of Neutralized Current Acid Waste from Double-Shell Tank 101-AZ*, PNL-7758; Pacific Northwest Laboratory: Richland, WA, 1989; https://www.osti.gov/scitech/servlets/purl/6277242.

(97) Poloski, A. P.; Daniel, R. C.; Rector, D. R.; Bredt, P. R.; Buck, E. C.; Berg, J. C.; Saez, A. E. *Characterization and Correlation of Particle-Level Interactions to the Macroscopic Rheology of Powders, Granular Slurries, and Colloidal Suspensions*, PNNL-16133; Pacific Northwest National Laboratory: Richland, WA, 2006; https://www.osti.gov/em52/2006projsum/90162.pdf.

(98) Rapko, B. M.; Lumetta, G. J.; Wagner, M. J. *Washing and Akaline Leaching of Hanford Tank Sludges: Results of FY 1995 Studies*, PNNL-10712; Pacific Northwest National Laboratory: Richland, WA, 1995; http://www.iaea.org/inis/collection/NCLCollectionStore/_Public/27/016/27016406.pdf.

(99) Rapko, B. M.; Wagner, M. J. *Caustic Leaching of Composite AZ-101/AZ-102 Hanford Tank Sludge*, PNNL-11580; Pacific Northwest National Laboratory: Richland, WA, 1997; https://www.osti.gov/scitech/servlets/purl/563223.

(100) Remund, K. M.; Tingey, J. M.; Heasler, P. G.; Toth, J. J.; Ryan, F. M.; Hartley, S. A.; Simpson, D. B.; Simpson, B. C. *Tank Characterization Report for Single-Shell Tank B-111*; PNL-10099; Pacific Northwest National Laboratory: Richland, WA, 1994; https://www.osti.gov/scitech/servlets/purl/10190375.

(101) Scheele, R. D.; Burger, R. L.; Sell, R. L.; Bredt, P. R.; Barrington, R. J. *Ferrocyanide Safety Project: Comparison of Actual and Simulated Ferrocyanide Waste Properties*, PNL-10175; Pacific Northwest National Laboratory: Richland, WA, 1994; http://www.iaea.org/inis/collection/NCLCollectionStore/_Public/26/050/26050959.pdf.

(102) Shimsky, R. W.; Billings, J. M.; Buck, E. C.; Casella, A. J.; Crum, J. V.; Daniel, R. C.; Draper, A. E.; Edwards, M. K.; Hallen, R. T.; Kozelisky, A. E.; MacFarlan, P. J.; Peterson, R. A.; Swoboda, M. P. *Filtration and Leach Testing for PUREX Cladding Sludge and REDOX Cladding Sludge Actual Waste Sample Composites*, PNNL-18048; Pacific Northwest National Laboratory: Richland, WA, 2009; http://www.pnl.gov/main/publications/external/technical_reports/PNNL-18048.pdf.

(103) Shimsky, R. W.; Billings, J. M.; Buck, E. C.; Daniel, R. C.; Draper, A. E.; Edwards, M. K.; Geeting, J. G. H.; Hallen, R. T.; Jenson, E. D.; Kozelisky, A. E.; MacFarlan, P. J.; Peterson, R. A.; Snow, L. A.; Swoboda, M. P. *Filtration and Leach Testing for REDOX Sludge and S-saltcake Actual Waste Sample Composites*, PNNL-17965; Pacific Northwest National Laboratory: Richland, WA, 2009; http://www.pnl.gov/main/publications/external/technical_reports/PNNL-17965.pdf.

(104) Simpson, B. C.; Borsheim, G. L.; Jenson, L. *Tank Characterization Report: Tank 241-C-109*, WHC-EP-0668, Rev. 0; Westinghouse Hanford Company: Richland, WA, 1993; https://www.osti.gov/scitech/servlets/purl/10103939.

(105) Temer, D. J.; Villarreal, R. *Sludge Washing and Alkaline Leaching Tests on Actual Hanford Tank Sludge: A status Report*, LA-UR-95−2070; Los Alamos National Laboratory: Los Alamos, NM, 1995; http://permalink.lanl.gov/object/tr?what=info:lanl-repo/lareport/LA-UR-95-2070.

(106) Temer, D. J.; Villarreal, R. *Sludge Water Washing and Alkaline Tests on Actual Hanford Tank Sludge: FY 1996 Results*, LA-UR-96−2839; Los Alamos National Laboratory: Los Alamos, NM, 1996; http://permalink.lanl.gov/object/tr?what=info:lanl-repo/lareport/LA-UR-96-2839.

(107) Temer, D. J.; Villarreal, R. *Sludge Water Washing and Alkaline Tests On Actual Hanford Tank Sludge: FY 1997 Results*, LA-UR-97−2889; Los Alamos National Laboratory: Los Alamos, NM, 1997; http://permalink.lanl.gov/object/tr?what=info:lanl-repo/lareport/LA-UR-97-2889.

(108) Urie, M. W.; Bredt, P. R.; Caldwell, D. D.; Farmer, O. T.; Fiskum, S. K.; Greenwood, L. R.; Hoppe, E. W.; Jagoda, L. K.; Mong, G. M.; Poloski, A. P.; Scheele, R. D.; Soderquist, C. V.; Swoboda, M. P.; Thomas, M. P.; Wagner, J. J. *Chemical Analysis and Physical Properties Testing of 241-AZ-101 Tank Waste Supernatant and Centrifuged Solids*, WTP-RPT-048, Rev. 1 (PNWD-3215 Rev. 1);

Battelle-Pacific Northwest Division: Richland, WA, 2004; http://www.pnl.gov/rpp-wtp/.

(109) Russel, W. B.; Saville, D. A.; Schowalter, W. R. *Colloidal Dispersions*; Cambridge University Press: New York, 1989.

(110) Hunter, R. J. *Foundations of Colloid Science*; Oxford University Press, 2001.

(111) Scales, P. J.; Johnson, S. B.; Healy, T. W.; Kapur, P. C. Shear yield stress of partially flocculated colloidal suspensions. *AIChE J.* **1998**, *44* (3), 538−544.

(112) Zhou, Z. W.; Scales, P. J.; Boger, D. V. Chemical and physical control of the theology of concentrated metal oxide suspensions. *Chem. Eng. Sci.* **2001**, *56* (9), 2901−2920.

(113) Ducker, W. A.; Senden, T. J.; Pashley, R. M. Direct measurement of colloidal forces using an atomic force microscope. *Nature* **1991**, *353* (6341), 239−241.

(114) Butt, H. J.; Cappella, B.; Kappl, M. Force measurements with the atomic force microscope: Technique, interpretation and applications. *Surf. Sci. Rep.* **2005**, *59* (1−6), 1−152.

(115) McKee, C. T.; Walz, J. Y. Interaction forces between colloidal particles in a solution of like-charged, adsorbing nanoparticles. *J. Colloid Interface Sci.* **2012**, *365* (1), 72−80.

(116) Shi, H.; Lercher, J. A.; Yu, X. Y. Sailing into uncharted waters: recent advances in the in situ monitoring of catalytic processes in aqueous environments. *Catal. Sci. Technol.* **2015**, *5* (6), 3035−3060.

(117) Morris, J. F. A review of microstructure in concentrated suspensions and its implications for rheology and bulk flow. *Rheol. Acta* **2009**, *48* (8), 909−923.

(118) Boek, E. S.; Coveney, P. V.; Lekkerkerker, H. N. W. Computer simulation of rheological phenomena in dense colloidal suspensions with dissipative particle dynamics. *J. Phys.: Condens. Matter* **1996**, *8* (47), 9509−9512.

(119) Sierou, A.; Brady, J. F. Accelerated Stokesian Dynamics simulations. *J. Fluid Mech.* **2001**, *448*, 115−146.

(120) Yeo, K.; Maxey, M. R. Numerical simulations of concentrated suspensions of monodisperse particles in a Poiseuille flow. *J. Fluid Mech.* **2011**, *682*, 491−518.

(121) Pednekar, S.; Chun, J.; Morris, J. F. Simulation of shear thickening in attractive colloidal suspensions. *Soft Matter* **2017**, *13* (9), 1773−1779.

(122) Burns, P. C. From extended solids to nano-scale actinide clusters. *C. R. Chim.* **2010**, *13* (6−7), 737−746.

(123) Rey, A.; Utsunomiya, S.; Gimenez, J.; Casas, I.; de Pablo, J.; Ewing, R. C. Stability of uranium (VI) peroxide hydrates under ionizing radiation. *Am. Mineral.* **2009**, *94* (2−3), 229−235.

(124) Chatterjee, S.; Conroy, M. A.; Smith, F. N.; Jung, H. J.; Wang, Z.; Peterson, R. A.; Huq, A.; Burtt, D. G.; Ilton, E. S.; Buck, E. C. Can Cr(III) substitute for Al(III) in the structure of boehmite? *RSC Adv.* **2016**, *6* (109), 107628−107637.

(125) Conroy, M.; Soltis, J. A.; Wittman, R. S.; Smith, F. N.; Chatterjee, S.; Zhang, X.; Ilton, E. S.; Buck, E. C. Importance of interlayer H bonding structure to the stability of layered minerals. *Sci. Rep.* **2017**, *7* (1), 13274.

DOI: 10.1021/acs.est.7b04077
Environ. Sci. Technol. 2018, 52, 381−396